

Autocrine activation of JAK2 by IL-11 promotes platinum drug resistance

Wei Zhou^{1,2,3,13}, Wei Sun^{4,13}, Mingo MH. Yung⁵, Sheng Dai^{2,4}, Yihua Cai^{1,3}, Chi-Wei Chen^{1,3}, Yunxiao Meng^{1,3}, Jennifer B. Lee^{1,3}, John C. Braisted⁴, Yinghua Xu⁶, Noel T. Southall⁴, Paul Shinn⁴, Xuefeng Huang², Zhangfa Song², Xiulei Chen⁷, Yan Kai^{3,9}, Xin Cai^{1,3}, Zongzhu Li^{1,3}, Qiang Hao^{1,3}, Annie NY. Cheung⁸, Hextan YS. Ngan⁸, Stephanie S. Liu⁸, Stephanie Barak¹⁰, Jing Hao¹, Zhijun Dai¹², Alexandros Tzatsos^{3,11}, Weiqun Peng⁹, Huadong Pei^{1,3}, Zhiyong Han¹, David W. Chan^{5,*}, Wei Zheng^{4,*}, Wenge Zhu^{1,3,*}

¹Department of Biochemistry and Molecular Medicine, The George Washington University School of Medicine and Health Sciences, Washington, DC 20037, USA.

²Department of Colorectal Surgery, Sir Run Run Shaw Hospital, School of Medicine, Zhejiang University, Hangzhou 310016, China.

³GW Cancer Centre, The George Washington University, Washington, DC 20052, USA.

⁴National Center for Advancing Translational Sciences, National Institutes of Health, Bethesda, MD 20892, USA.

⁵Department of Obstetrics and Gynecology, LKS Faculty of Medicine, The University of Hong Kong, Hong Kong SAR, China.

⁶Department of Medical Oncology, Sir Run Run Shaw Hospital, School of Medicine, Zhejiang University, Hangzhou 310016, China.

⁷Department of Clinical Laboratory, Sir Run Run Shaw Hospital, School of Medicine, Zhejiang University, Hangzhou 310016, China.

⁸Department of Pathology, LKS Faculty of Medicine, The University of Hong Kong, Hong Kong SAR, China.

⁹Department of Physics, The George Washington University Columbian College of Arts & Sciences, Washington, DC 20052, USA.

¹⁰Department of Pathology, The George Washington University School of Medicine and Health Sciences, Washington, DC 20037, USA.

¹¹Department of Anatomy and Regenerative Biology, The George Washington University School of Medicine and Health Sciences, Washington, DC 20037, USA.

¹²Department of Oncology, the Second Affiliated Hospital, Xi'an Jiaotong University, Xi'an 710004, China.

¹³Co-first authors.

* Co-corresponding authors:

David W Chan, Tel: (852) 39179367; Email: dwchan@hku.hk

Wei Zheng; Tel: 301-217-5251, Email: wzheng@mail.nih.gov

Wenge Zhu (contact), Tel: 202-994-3125; Email: wz6812@gwu.edu

Running Title: IL-11- JAK2 promotes platinum drug resistance

Abstract

Antineoplastic platinum agents are used in first-line treatment of ovarian cancer, but treatment failure frequently results from platinum drug resistance. Emerging observations suggest a role of reactive oxygen species (ROS) in the resistance of cancer drugs including platinum drugs. However, the molecular link between ROS and cellular survival pathway is poorly understood. Using quantitative high throughput combinational screen (qHTCS) and genomic sequencing, we show that in platinum resistant ovarian cancer elevated ROS levels sustain high level of IL-11 by stimulating FRA1-mediated IL-11 expression and increased IL-11 causes resistance to platinum drugs by constitutively activating JAK2-STAT5 via an autocrine mechanism. Inhibition of JAK2 by LY2784544 or IL-11 by anti-IL-11 antibody overcomes the platinum resistance *in vitro* or *in vivo*. Significantly, clinic studies also confirm the activated IL-11-JAK2 pathway in platinum-resistant ovarian cancer patients, which highly correlates with poor prognosis. These findings not only identify a novel ROS-IL-11-JAK2-mediated platinum resistance mechanism but also provide a new strategy for using LY2784544 or IL-11-mediated immunotherapy to treat platinum-resistant ovarian cancer.

Keywords: JAK2/IL-11/platinum drug/cisplatin resistance/ovarian cancer

Introduction

Ovarian cancer is the fifth leading cause of cancer-related death among women and the deadliest gynecological cancer in the United States ³¹. The current standard treatment for ovarian cancer consists of surgery followed by platinum drug based chemotherapy ^{15, 21}. Platinum drugs act by entering the nucleus of the cell and forming covalent adducts with DNA, thus decreasing cell viability ⁷. In addition to nuclear DNA damage, cisplatin can induce reactive oxygen species (ROS) response that can significantly enhance the cytotoxic effect ^{5, 20}. Up to 80% of patients with ovarian cancers initially respond to cisplatin-based chemotherapy and achieve remission ^{1, 4}. However, cancer relapse occurs in about 80% of patients, and the relapsed ovarian cancer patients are more resistant to platinum-based therapy ¹¹. Studies in the past characterized a plethora of mechanisms for cisplatin resistance, including reduced intracellular cisplatin accumulation, increases in metabolic inactivation of cisplatin, repair of cisplatin-induced DNA damage, and inactivation of p53 ^{10, 36}. Emerging observations also indicated a role of ROS in cisplatin resistance ³⁴. However, the detailed molecular mechanism of how ROS contributes to platinum drug resistance by regulating cell survival pathway remains largely unknown.

Janus kinase 2 (JAK2) is a member of the Janus kinase family, which contains JAK1, JAK2, JAK3 and tyrosine kinase 2 (TYK2). JAKs are recruited to cellular membrane and activated by cytokine-activated receptors ²⁸. Activated JAKs phosphorylate and activate signal transducer and activator of transcription (STAT) factors, which then translocate to nucleus to regulate the expression of genes involving in cell proliferation and apoptosis ²⁹. Interleukin-11 (IL-11) is a member of the GP130 family that includes IL-6, IL-27, IL-31, OSM and LIF ³. IL-11 binds to the transmembrane receptor IL-11 R α , causing activation of JAK2 and hence the downstream STAT pathway ^{2, 9}. However, the role of IL-11 in the response of cancer cells to chemotherapy remains largely unknown.

In this study, for the first time, we provided an unbiased high throughput analysis to study platinum drug resistance in ovarian cancer by combined use of quantitative high-throughput combinational screening (qHTCS) and genomic sequencing techniques. The advantage of this approach is that it not only identifies novel drug combinations to treat drug resistance cancers but also discovers novel drug resistant mechanisms that cannot be identified by each technique alone.

Indeed, we identified LY2784544, a JAK2 inhibitor under phase II clinical trial for myeloproliferative neoplasms¹⁹, to be an effective drug to efficiently resensitize platinum drug resistant ovarian cancer *in vitro* and *in vivo*. Detailed mechanistic analyses indicated that in platinum-resistant ovarian cancer cells ROS promotes FRA1-dependent expression of IL-11, resulting in constitutive activation of JAK2-STAT5 pathway and resistance to platinum drugs. Most importantly, this novel mechanism is supported by our clinic findings: JAK2 activation correlates with high levels of IL-11 in the most tested platinum resistant ovarian tumors and the activated IL-11-JAK2 pathway is correlated with a low overall survival rate of ovarian cancer patients receiving platinum drug-based chemotherapy.

Results

Establishment of platinum resistant ovarian cancer cells

The objective of this study is to conduct both qHTCS and genomic sequencing using platinum drug resistant ovarian cancer cells to discover new mechanisms of resistance as well as novel drug combinations that can overcome platinum drug resistance (Fig. 1A). To accomplish this objective, we first established cisplatin resistant ovarian cancer cells using procedures as described previously and in methods¹³. Specifically, starting with two ovarian cancer cell lines (SKOV3 and IGROV1), we obtained sub-cell lines, called SKOV3 CR and IGROV1 CR, that were able to grow in the medium containing a high concentration of cisplatin (Fig. 1B). Subsequent cell viability analyses revealed that the IC₅₀ of cisplatin for SKOV3 CR was increased by 5-fold and IC₅₀ of cisplatin for IGROV1 CR by 3-fold (Fig. 1B). SKOV3 CR cells were also resistant to carboplatin (Supplementary Fig. 1A), which is also used to treat ovarian cancer patients clinically²⁵. Apoptosis analyses indicated that cisplatin induced more apoptosis in SKOV3 cells than in SKOV3 CR cells (Supplementary Fig. 1B and 1C). Significantly, *in vivo* studies indicated that SKOV3 CR tumor was more resistant to cisplatin than SKOV3 tumor through anti-apoptosis (Supplementary Fig. 1D).

We next measured the DNA crosslinking in both cells post cisplatin treatment using a modified comet assay and found that there was no difference in the extent of cisplatin-DNA crosslinking between SKOV3 and SKOV3 CR cells²³ (Supplementary Fig. 1 E). Thus, SKOV3 CR cells

remain susceptible to cisplatin-induced DNA damage and it is unlikely that there are defects in cisplatin uptake.

Identification of LY2784544 that overcomes cisplatin resistance via a qHTCS

We employed these cells in a qHTCS to identify novel drug combinations to re-sensitize the cells to cisplatin. To this end, we screened a total of 6,016 compounds from multiple compound libraries including NPC (NCGC Pharmaceutical Collection), MIPE (Mechanism Interrogation Plate) and LOPAC (The Library of Pharmacologically Active Compounds). Two rounds of qHTCS screen were performed (Supplementary Fig. 2A). From the first screen, we identified a total of 112 compounds that efficiently inhibited the proliferation of SKOV3 CR cells (Supplementary Fig. 2B). To further identify compounds that have synergy with cisplatin, these 112 compounds were screened at 11 different concentrations in combination with vehicle, 1 μ M cisplatin or 20 μ M cisplatin (Fig. 1C and Supplementary Fig.2A). Through this second screen, thirteen compounds that improved the cytotoxicity of cisplatin in SKOV3 CR cells were identified (Supplementary Table S1). In the next screen, cisplatin was tested at 11 different concentrations from 0.046 to 47 μ M in combinations with these thirteen compounds (Supplementary Fig.2A). Three compounds, LY2784544 (JAK2 inhibitor), MLN4924 (NEDD8 inhibitor) and NSC319726 (p53 mutant reactivator), were found to have significant reciprocal synergy with cisplatin on SKOV3 CR cells (Fig. 1C).

Among the three compounds, LY2784544 has better cisplatin IC₅₀ shift ability than MLN4924 or NSC319726, which significantly increased the sensitivity of SKOV3 CR cells to cisplatin to a degree similar to SKOV3 cells (Supplementary Fig. 2C, left panel). Cisplatin sensitized SKOV3 CR cells to LY2784544 reciprocally (Supplementary Fig. 2C, right panel). The synergistic effects of MLN4924 or NSC319726 on cisplatin resistant ovarian cancer cells have been reported independently by other groups^{13, 38}, validating the use of this qHTCS to identify compounds overcoming cisplatin resistance. In subsequent studies, we mainly focused on investigating the mechanism by which LY2784544 overcomes cisplatin resistance of ovarian cancer cells.

JAK2 inhibition synergizes with platinum drugs in platinum resistant ovarian cancer cells

We conducted multiple analyses to confirm the synergistic effects of LY2784544 with cisplatin in cisplatin resistant SKOV3 CR cells. First, we measured cell proliferation using sulforhodamine

B (SRB) assay(and calculated the synergy between LY2784544 and cisplatin using Combeneft⁸, and found excellent synergy in SKOV3 CR cells compared to that in SKOV3 cells (Fig. 1D and Supplementary Fig. 3A). We also calculated the combination index (CI), which quantitatively measures the interaction between two drugs (synergism: CI < 1; additive effect: CI = 1; and antagonism CI > 1)⁶. Significantly, the combination of cisplatin and LY2784544 exhibited excellent synergy on SKOV3 CR cells (mean CI = 0.69) and additive effect on SKOV3 cells (mean CI = 0.93) (Supplementary Fig. 3B). Using similar analysis, the combination of cisplatin and LY2784544 also had an excellent synergy (mean CI = 0.71) on IGROV1 CR cells (Fig. 1E).

Given that both SKOV3 CR and IGROV1 CR cells acquired resistance under a cell culture condition, we next examined the synergy of LY2784544 and cisplatin in a paired ovarian cancer cells, PEO1 and PEO4, derived directly from one patient before and after chemotherapy¹⁷. PEO1 cells are platinum sensitive and PEO4 cells are platinum resistant cells. We did find that the IC₅₀ of cisplatin for PEO4 cells was increased by 3-fold compared to that for PEO1 cells (Fig. 1F). Importantly, the combination of cisplatin and LY2784544 exhibited excellent synergy (mean CI = 0.34) in PEO4 cells (Fig. 1G).

Using a clonogenic assay, we found that SKOV3 CR cells exhibited a higher survival rate compared to SKOV3 cells after a cisplatin treatment. Combinatorial treatment with cisplatin plus LY2784544 significantly reduced the survival of SKOV3 CR compared to cisplatin or LY2784544 treatment alone (Supplementary Fig. 3C). We also examined the synergy of LY2784544 with carboplatin in SKOV3 CR cells. Consistently, the combination of carboplatin and LY2784544 also exhibited an excellent synergistic effect (mean CI = 0.75) on SKOV3 CR cells (Supplementary Fig. 3D).

To confirm the JAK2 inhibitor's effect on synergy with cisplatin, we next tested other two JAK2 inhibitors, TG101348 and TG-46. Similarly, both showed a synergistic effect with cisplatin on SKOV3 CR cells (Supplementary Fig. 3E and S3F). Taken together, our data strongly demonstrate a general synergistic effect of JAK2 inhibitors with platinum drugs on platinum drug resistant ovarian cancer cells.

LY2784544 overcomes cisplatin resistance of ovarian cancer cells by inhibiting JAK2-mediated pathways in vitro and in vivo

We next explored the molecular mechanism by which the JAK2 signaling pathway confers cisplatin resistance in ovarian cancer. We first examined the activation of the JAK2-mediated pathway in three pairs of cisplatin sensitive (SKOV3, IGROV1, PEO1) and resistant (SKOV3 CR, IGROV1 CR, PEO4) cell lines. Compared to the three sensitive cell lines, the JAK2 protein levels were not altered in paired resistant cell lines (Fig. 2A). Strikingly, phosphorylation of JAK2 at Y1007/1008 significantly increased in all resistant cells compared to their sensitive counterparts. Consistent with the activation of JAK2, we found the phosphorylation of STAT5 (Y694), a downstream target of JAK2^{19,37}, was increased in all three resistant cell lines (Fig. 2A). The downregulation of JAK2 by shRNA significantly sensitized the SKOV3 CR cells to cisplatin (Fig. 2B and C), confirming that the cisplatin resistance in SKOV3 CR is JAK2-dependent.

We next examined the effects of LY2784544 on the JAK2-STAT5 signaling pathway in both SKOV3 and SKOV3 CR cells. Apparently, LY2784544 significantly reduced the phosphorylation of both JAK2 and STAT5 in both SKOV3 and SKOV3 CR cells (Fig. 2D). Treatment of SKOV3 CR cells with LY2784544 efficiently decreased the activation of JAK2 and STAT5 but did not cause apoptosis as evidenced by a lack of cleaved PARP (Fig. 2E). However, the combination of cisplatin and LY2784544 not only reduced the phosphorylation of JAK2 and STAT5 but also enhanced apoptosis (Fig. 2E and F and Supplementary Fig. 4A).

To determine whether LY2784544 can sensitize SKOV3 CR cells to cisplatin *in vivo*, we subcutaneously implanted SKOV3 CR cells into nude mice to form tumors, followed by various treatments. Although SKOV3 CR tumors were resistant to cisplatin or LY2784544, the combinatorial treatment with cisplatin and LY2784544 significantly not only reduced tumor growth (Fig. 2G), but also improved survival of the mice with SKOV3 CR tumors (Fig. 2H). To evaluate the efficacy of this combinational treatment and whether this *in vivo* tumor suppression was mediated through inhibition of JAK2, we collected SKOV3 CR xenograft tumor samples four days after full dosage treatment. Immunohistochemistry (IHC) analyses indicated that LY2784544 treatment efficiently reduced the phosphorylation of JAK2 and the treatment with LY2784544 plus cisplatin significantly induced apoptosis in the tumor as indicated by TUNEL staining (Fig. 2 I-K). To evaluate the toxicity of treatment of cisplatin plus LY2784544 in mice, we carefully monitored the weight of the mice throughout the treatments and found that there was no significant reduction in

body weight during the whole treatment period (Supplementary Fig. 4B). No obvious histopathological alterations and lesions were found in liver and kidney of the treated animals (Supplementary Fig. 4C).

The LY2784544 was reported as a selective JAK2 inhibitor¹⁹. To confirm the selectivity of LY2784544, we conducted an *in vitro* kinase profiling to exam the interaction of LY2784544 with more than 450 human kinases. The results showed that LY2784544 exhibited stronger binding to JAK2 than JAK1 and TYK2 (Supplementary Fig. 4D), indicating the high selectivity of LY2784544 towards JAK2.

Identification of IL-11 as a key factor that regulates JAK2 activity in vitro and in vivo

We next investigated how JAK2 is activated in cisplatin resistant ovarian cancer cells. Given that JAK2 could be constitutively activated by mutations including the V617F mutation^{12, 16, 18, 22, 30}, we first sequenced and compared the *JAK2* gene in SKOV3 and SKOV3 CR cells (Supplementary Fig. 5A). However, we did not find any mutations in the *JAK2* gene in SKOV3 CR cells.

Since cytokine-activated receptors can regulate the activation of JAK2^{3, 24, 26, 35}, we hypothesized that secreted factors in the medium of SKOV3 CR cells might cause, in an autocrine fashion, activation of JAK2, resulting in resistance to cisplatin. To test this possibility, we collected conditioned medium from SKOV3 CR cells and then used the medium to culture SKOV3 cells. Strikingly, SKOV3 cells cultured in the conditioned medium from SKOV3 CR displayed an increased resistance to cisplatin compared to cells cultured in the conditioned medium from SKOV3 (Fig. 3A), indicating that secreted factors from SKOV3 CR cells caused the cisplatin resistance of SKOV3 cells. Strikingly, SKOV3 cells cultured in the conditioned medium from SKOV3 CR cells activated JAK2 and STAT5 (Fig. 3B).

To identify the cytokine factors in the conditioned medium from SKOV3 CR cells that active JAK2, we screened the cytokine levels in the conditioned medium of SKOV3, SKOV3 CR, PEO1, and PEO4 cells using a cytokine array. The result indicated significantly elevated levels of four cytokines (Eotaxin-2, Eotaxin-3, IL-11, and uPAR) in the medium of both SKOV3 CR and PEO4 cells compared with their parental cells (Fig. 3C and D). Furthermore, we also examined and compared gene expression profiles between SKOV3 and SKOV3 CR cells. There was a total of 1085 up-regulated

genes and 1686 down-regulated genes in SKOV3 CR compared to SKOV3 cells (Fig. 3 E). Comparing the genes in the cytokine pathways, we found that a total of 74 genes are either up- or down-regulated (more than 2-fold change) in SKOV3 CR cells (Fig. 3F). We then compared these four cytokine genes with 30 up-regulated cytokine genes identified by genomic sequencing as well as 155 genes involving in KEGG JAK/STAT signaling pathway (Pathway: map04630), and found that IL-11 is the only up-regulated cytokine that is most likely to cause activation of JAK pathway in platinum drug resistant ovarian cancer cells (Fig. 3G). We therefore analyzed and compared IL-11 mRNA levels by qPCR in sensitive and resistant cells and found that IL-11 mRNA levels increased significantly in all three resistant cell lines (Fig. 3H). Consistently, the amounts of secreted IL-11 proteins in the medium of all three resistant cells were significantly higher than that in the medium of their sensitive counterparts (Fig. 3I). To rule out the possibility that JAK2-STAT5 activation in the resistant cells might be due to the overexpression of IL-11 receptors, we next examined the expression of subunits of IL-11 receptor, including IL-11R α , IL-6R α , EPOR and G-CSFR, in SKOV3 and SKOV3 CR cells, and found that the levels of each protein did not increase in SKOV3 CR compared to SKOV3 cells (Supplementary Fig. 5B).

Given that both IL-11 mRNA and IL-11 protein are increased in the resistant cells, we hypothesized that IL-11 might also be up-regulated in cisplatin resistant ovarian tumors *in vivo*. To test this hypothesis, we examined the levels of IL-11 protein in SKOV3 and SKOV3 CR tumors by IHC and found that IL-11, as well as levels of phosphorylation of JAK2, were significantly increased in SKOV3 CR xenograft tumor cells (Supplementary Fig. 5C and 5D). Taken together, our results indicate that IL-11 levels are up-regulated in cisplatin resistant cancer cells *in vitro* and *in vivo*.

Autocrine activation of IL-11 promotes cisplatin resistance by regulating JAK2-STAT5 activation in ovarian cancer cells

The above findings suggested that IL-11 might be a critical factor contributing to cisplatin resistance by stimulating JAK2 activity in ovarian cancer cells. Therefore, we first tested whether IL-11 can stimulate the activation of JAK2 in SKOV3 cells. Indeed, recombinant IL-11 treatment increased the phosphorylation of JAK2 and STAT5 (Fig. 4A). To support the notion that IL-11 contributes to cisplatin resistance in ovarian cancer cells, we found that treatment of SKOV3 with recombinant IL-11 induced resistance to cisplatin (Fig. 4B). When IL-11 neutralization antibody was

added to the culture medium of SKOV3 CR and IGROV1 CR, we observed reduced phosphorylation of JAK2 and STAT5 (Fig. 4C), and increased the sensitivity of the cells to cisplatin (Fig. 4D, upper panel, SKOV3 CR; lower panel, IGROV1 CR). Thus, secreted IL-11 acts as an autocrine factor to stimulate the activation of the JAK2-STAT5 pathway, thereby inducing cisplatin resistance in these cells.

To further test the relationship between IL-11 and cisplatin resistance in ovarian cancer cells, we depleted *IL-11* by shRNA in SKOV3 CR cells and found that downregulation of *IL-11* not only decreased the IL-11 secretion (Fig. 4E) but also reduced the activation of JAK2 and STAT5 (Fig. 4F). More significantly, depletion of IL-11 re-sensitized SKOV3 CR cells to cisplatin (Fig. 4G). Addition of recombinant IL-11 to the medium restored the cisplatin resistance of SKOV3 CR cells with downregulated IL-11 by shRNA (Fig. 4H), indicating that reduced resistance by IL-11 depletion is not due to the shRNA off-target effect. To further confirm that IL-11-induced cisplatin resistance is JAK2-dependent, we downregulated JAK2 by siRNA in SKOV3 cells with recombinant IL-11 for four hours and then cisplatin treatment for five days (Fig. 4I). Although the addition of recombinant IL-11 could induce resistance to cisplatin in cells containing JAK2, IL-11 no longer induced cisplatin resistance in the cells with downregulated JAK2 (Fig. 4I). These findings indicate that JAK2 signaling is a major mechanism involved in IL-11-induced cisplatin resistance in SKOV3 cells.

Cisplatin induces IL-11-mediated autocrine activation of JAK2-STAT5 in vitro and in vivo

We next explored the molecular mechanism of how ovarian cancer cells acquire resistance to cisplatin during cisplatin treatment, which can explain how ovarian cancer patients develop resistance to platinum drugs after receiving platinum-based therapy.

Given that the elevated IL-11 stimulates JAK2 activation to induce cisplatin resistance, it is highly possible that cisplatin may result in increased expression and secretion of IL-11 as a compensatory surviving mechanism. To avoid cell death, we treated cells with cisplatin less than 50% of IC_{50} . Indeed, the small dosage of cisplatin treatment increased secretion of IL-11 in SKOV3 cells, and furthermore, IL-11 secretion appeared to be dependent on cisplatin doses and treatment time (Fig. 5A). *IL-11* mRNA levels were also increased in cells following cisplatin

treatment (Fig. 5B), indicating that elevated secretion of IL-11 is due to up-regulated expression of *IL-11* gene. As expected, JAK2 and STAT5 were activated after cisplatin treatment (Fig. 5C).

To further test whether ovarian cancer cells have a similar response to cisplatin *in vivo*, we treated SKOV3 xenograft tumor with various doses of cisplatin for 2 weeks (Fig. 5D). Four days after the last treatment, blood and tumor samples were collected for analyses of IL-11 levels. Significantly, cisplatin treatment dramatically increased human IL-11 levels in the serum of mice (Fig. 5E). IHC analysis indicated a significant increase of IL-11 as well as pJAK2 levels in SKOV3 tumors (Fig. 5F). Interestingly, the levels of both IL-11 and pJAK2 in the tumors were dependent on cisplatin doses: the higher the cisplatin dose the higher the levels of IL-11 and pJAK2 (Fig. 5G). Thus, cisplatin treatment induces the activation of the IL-11-JAK2 pathway in tumor cells *in vivo* as well. These results provide *in vivo* and *in vitro* evidence that may explain how ovarian cancer patients develop IL-11-JAK2-mediated platinum drug resistance.

ROS induces autocrine activation of IL-11 by promoting expression of FOSL1 (FRA1)

The next question is how IL-11 is activated in platinum drug resistant ovarian cancer cells. Since DNA damage induces ROS generation^{14,33}, we next investigated whether ROS is involved in up-regulation of IL-11. To this end, we first compared ROS level between SKOV3 and SKOV3 CR cells. Strikingly, the basal ROS level in SKOV3 CR cells was significantly higher than that in SKOV3 cells (Fig. 6A). To investigate if ROS in SKOV3 CR cells regulate IL-11 expression, we treated SKOV3 CR cells with a ROS inhibitor YCG063 and found that inhibition of ROS significantly reduced IL-11 secretion as well as JAK2 and STAT5 phosphorylation (Fig. 6B-D and Supplementary Fig. 6A), indicating that ROS is critical for the secretion of IL-11 in cisplatin resistant cells. Next, we treated SKOV3 cells with cisplatin, YCG063 or in combination. Cisplatin treatment alone remarkably activated ROS production while YCG063 suppressed it in SKOV3 cells (Fig. 6E and Supplementary Fig. 6B). Furthermore, inhibition of ROS in SKOV3 cells suppressed the cisplatin-induced IL-11 secretion (Fig. 6F), phosphorylation of JAK2 and STAT5 (Fig. 6G).

Having found that the ROS regulates IL-11 secretion, we then decided to identify critical ROS responsive genes that regulate *IL-11* expression. To achieve this goal, we first conducted pathway analyses using PathwayNet and identified a total of 20 transcription factors that likely regulate *IL-11*²⁷(Fig. 6H). By comparing these candidate genes with the genes identified from RNA-

Seq analyses, we found that the *FOSL1* is the only gene that is significantly up-regulated by more than 2-fold in SKOV3 CR cells (Fig. 6H). Further analyses indicated that the levels of *FOSL1*-encoded protein, FRA1, and phosphorylated (Ser265) FRA1 were increased in SKOV3 CR cells compared to SKOV3 cells (Fig. 6I). Depletion of FRA1 by *FOSL1* siRNA significantly reduced IL-11 secretion in SKOV3 CR cells (Fig. 6J and K), indicating that FRA1 is critical for IL-11 expression. We next tested whether ROS is required for activation or expression of FRA1 by treating SKOV3 CR cells with YGC063. Significantly, inhibition of ROS reduced the expression of FRA1 as well as its phosphorylation (Fig. 6L), indicating that the ROS signaling is required for the activation of FRA1.

Clinical evidence of activated IL-11-JAK2 pathway in platinum drug resistant ovarian cancer patients

To investigate and confirm the role of the IL-11-JAK2 pathway in platinum drug resistance of ovarian cancer patients, we first compared the IL-11 mRNA levels from patient samples of a total of 23 platinum sensitive patients and 16 resistant patients (Supplementary Table S2). We found that IL-11 levels in the platinum drug-resistant group are higher than that in sensitive group (Fig. 7A). Significantly, the group of patients with higher mRNA levels of IL-11 exhibited worse prognosis in terms of PFS and OS than the group with low mRNA *IL11* level (Supplementary Fig. 7A). We also examined and compared the serum IL-11 levels from a total of 21 platinum sensitive patients and 16 resistant patients (Supplementary Table S3). We found that the platinum drug-resistant group had a mean level of 120.2 pg/ml of serum IL-11, which is significantly higher than the platinum drug sensitive group (22.8 pg/ml of IL-11) (Fig. 7B). Also, the group of patients with higher serum levels of IL-11 (≥ 40 pg/ml) exhibited worse prognosis in terms of PFS and OS (Fig. 7C) than the group with low serum IL-11 level (< 40 pg/ml), indicating an inverse correlation between the serum levels of IL-11 and the survival rate of ovarian patients following platinum drug-based therapy. Out of these 37 patients, we identified one patient with both sensitive and resistant samples. The resistant tumors exhibited higher levels of IL-11 and p-JAK2 expression (Fig. 7D and Supplementary Table S4).

We also evaluated the correlation of the IL-11-JAK2 pathway in the samples from the same patient before platinum drug treatment and after tumor recurrence. We identified a total of seven patients who have received platinum drug based chemotherapy and had a recurrence 11-41

months post treatment (Supplementary Table S4). IHC staining indicated that IL-11 levels were increased in four of seven (57.1%) patients (Fig. 7E and Supplementary Fig. 7B). Strikingly, there was a significant correlation between IL-11 and pJAK2 levels in all tested primary and recurrent patient tumor samples (Fig. 7F).

To further investigate the role of JAK2 activation in the regulation of platinum drug resistance in ovarian cancer, we next examined the correlation of the JAK2 activity with ovarian patient survival rate using large scaled ovarian cancer data bases. Since JAK2 phosphorylation but not proteins levels are up-regulated in platinum resistant cells, we therefore investigated the correlation of the JAK2 pathway with cisplatin resistance by analyzing and comparing the JAK2-regulated functional pathways and gene expression profiles obtained from genomic sequencing. Specifically, we first analyzed the genes that are functionally linked with JAK2 by using PathwayNet and identified a total of 500 genes linked to JAK2 activity. Analyzing gene expression from RNA-Seq data, we identified a total of 1085 genes that are up-regulated at least 2-fold in SKOV3 CR compared to SKOV3 cells (Fig. 3E). Comparing these two sets of genes, we found a total of 22 overlapped genes (Fig. 7G), which we named as JAK2 signature genes. Given that JAK2 activity is up-regulated in cisplatin resistant cells, we hypothesized that the levels of these JAK2 signature genes should inversely correlate to survival rate. We analyzed and compared JAK2 signature genes from 1816 patients found in 15 datasets using a Kaplan-Meier plotter³². Indeed, patients with platinum drug treatment history exhibited a worse 5-year PFS and OS when JAK2 signature genes expression levels in their tumors were higher (Fig. 7H). Thus, a higher activity of the JAK2 pathway is highly correlated with worse ovarian cancer patient survival following platinum drug-based therapy.

Discussion

In this study, we have demonstrated that qHTCS is an unbiased and quick method to study platinum drug resistance in ovarian cancer. The advantage of using such an approach is that it not only quickly identifies novel drug combinations in an unbiased manner but also the most likely drug target proteins and signal transduction pathways, especially those with post-transcriptional modification such as this JAK activation-mediated pathway. Specifically, we have successfully

identified that the elevated ROS production is responsible for activation of the IL-11-mediated autocrine mechanism that activates JAK-2-STAT5 signal transduction pathway to endow the ovarian cancer cells with cisplatin resistance (Supplementary Fig. 7C, left panel). Furthermore, targeting JAK2 or IL-11 can re-sensitize platinum drug resistant ovarian cancer cells to the platinum drug (Supplementary Fig.7C, right panel). Importantly, this novel molecular mechanism of platinum resistance has been confirmed by clinical studies. Thus, tumors with elevated IL-11 production and JAK2 activity in patients are more likely to exhibit cisplatin resistance and patients with such tumors have a poor prognosis following platinum-based therapy.

LY2784544 is currently investigated in clinical Phase 2 trial for its potential to treat myeloproliferative neoplasms (NCT01594723). Our studies indicate that LY2784544 can efficiently sensitize platinum resistant ovarian cancer cells to cisplatin both in *vitro* and in animals due to its ability to inhibit JAK2, thereby blocking the IL-11 autocrine mechanism for platinum resistance. Therefore, the use of specific JAK2 inhibitors, such as LY2784544, is likely to lead to a promising, more efficient combinatorial chemotherapy with platinum drugs as the first-line treatment for ovarian cancers or to treat relapsed ovarian cancer patients after platinum-based chemotherapy. Nevertheless, future clinical trials are needed to evaluate the safety and efficacy of the combination of platinum drugs and LY2784544 or other JAK2 inhibitors for ovarian cancer treatment.

The discovery of an IL-11 autocrine mechanism that activates JAK2 and signals transduction to induce platinum drug resistance in ovarian cancer cells is exciting because it explains why ovarian cancer patients with high serum and tumor levels of IL-11 exhibit poor prognosis compared to those with low serum and tumor IL-11 levels. It is striking that elevated ROS levels are required to sustain high levels of IL-11 via regulating the expression of FRA1 (Fig. 6L). The ROS signaling can cause elevated expression of survival factors such as BCL-2 and MCL1 and decrease levels of cell death factors³⁴. However, the detailed molecular mechanism of how ROS regulates these factors is unknown. Thus, for the first time our studies provide a novel mechanism by which ROS promotes cell survival through stimulating FRA1-mediated expression of IL-11 in ovarian cancer cells to promote, in an autocrine fashion, their resistance to platinum drugs

Our clinical findings indicate that platinum drug treatment of patients does increase the serum levels of IL-11, which is consistent with our findings in animals. Thus, this study suggests a

new strategy to increase the efficacy of platinum-based therapy for ovarian cancer and may be for other cancer types – that is, to develop and use agents, such as humanized monoclonal antibodies against IL-11 and/or IL-11R α , to sensitize platinum resistant ovarian cancer to platinum drugs again. However, since cisplatin treatment stimulates the expression of IL-11 in tumor cells, there is more reason to consider the combined use of a platinum drug with an agent that targets IL-11 or IL-11R α to prevent cancer cells from acquiring resistance to the platinum drugs during treatment. Given that we can monitor the serum IL-11 level in patients, measurement of serum IL-11 level also provides us with a useful biomarker to evaluate the potential resistance of patients to platinum drugs. However, this hypothesis needs to be carefully evaluated using a large cohort of ovarian cancer patients in future studies.

Materials and Methods

Cell lines and resistance cell line establishment The human ovarian cancer cell line SKOV3 was obtained from the American Type Culture Collection (ATCC). PEO1, PEO4, and PEA1 were from Sigma-Aldrich. IGROV1 was a kind gift from Wei Zheng. SKOV3 cells were cultured in McCoy's 5A Medium supplemented with 10% fetal bovine serum (FBS). A2780, IGROV1, PEO1, PEO4, and PEA1 cells were cultured in RPMI-1640 supplemented with 10% FBS. The cisplatin resistant cell line SKOV3 CR and IGROV1 CR were generated by treated with cisplatin for six cycles (4 hr cisplatin treatment, followed by release to cisplatin free medium for three weeks). Only early-passage (< 10 passages) resistant cells were used for the study. All cells were cultured at 37 °C in a humidified incubator containing 5% CO₂.

Quantitative high-throughput combinational screening (qHTCS) Compound screening experiments were performed as previously described³².

Cell viability assay Cell viability was determined by a sulforhodamine B (SRB) assay as described previously³⁷.

Animal experiments The detailed procedure of animal experiments is provided in Supplementary data.

Cytokine array Cytokine arrays on cell culture medium were performed using the Human Cytokine Antibody Array Kit (Abcam, 120 Targets) according to the manufacturer's protocol. Single intensity was analyzed using ImageJ (NIH) software. The results were then normalized using internal controls, and the relative protein levels were determined across four biological replicates.

ELISA The cell-free culture medium, mouse serum, and patient serum were analyzed for IL-11 levels using a human IL-11 ELISA kit (R&D Systems) according to the manufacturer's instructions. The absorbance was read at 450 nm using a microplate reader (BioTek). The data were normalized to the cell number.

Reactive oxygen species (ROS) detection ROS was detected with a live cell-permeable, fluorophore CellROX Orange reagent (Thermo Fisher Scientific) according to the manufacturer's instructions. After treatment, cells were incubated with CellROX Orange reagent and Hoechst (Thermo Fisher Scientific) at 37 °C for 30 min, followed by washing twice with prewarmed PBS. Cells were imaged using a Nikon Eclipse 80i microscope. ROS intensity was analyzed using ImageJ (NIH) software.

Patients The detailed information on human patients is provided in Supplementary data.

Statistical analysis Each value reported represents the mean \pm standard error of the mean (SEM) or mean \pm standard deviation (SD) as noted in the figure legends. A Student's t-test was used to analyze differences in tumor volumes between two groups. For comparisons between multiple groups, a one-way ANOVA or two-way analysis was used with a Bonferroni post-test. For Kaplan Meier survival analysis, a Log-rank (Mantel-Cox) test was used to compare each of the arms. All statistical tests were two-sided. Differences were considered statistically significant at a P value of less than 0.05. All statistical analyses were performed with GraphPad Prism, software version 7.00.

Conflicts of Interest

No potential conflicts of interest.

Acknowledgements

This work was partially supported by funding from the National Institutes of Health (CA177898 and CA184717 to Z.W.), the McCormick Genomic and Proteomic Center, and intramural research

program at the National Center for Advancing Translational Sciences (NCATS). Wenge Zhu was supported by a Research Scholar Grant, RSG-13-214-01-DMC from the American Cancer Society. This work was supported by the National Natural Science Foundation of China grant 81402580 to W. Zhou.

References

- 1 Armstrong DK, Bundy B, Wenzel L, Huang HQ, Baergen R, Lele S *et al.* Intraperitoneal cisplatin and paclitaxel in ovarian cancer. *N Engl J Med* 2006; 354: 34-43.
- 2 Bromberg J. Stat proteins and oncogenesis. *J Clin Invest* 2002; 109: 1139-1142.
- 3 Buchert M, Burns CJ, Ernst M. Targeting JAK kinase in solid tumors: emerging opportunities and challenges. *Oncogene* 2016; 35: 939-951.
- 4 Burger RA, Brady MF, Bookman MA, Fleming GF, Monk BJ, Huang H *et al.* Incorporation of bevacizumab in the primary treatment of ovarian cancer. *N Engl J Med* 2011; 365: 2473-2483.
- 5 Choi YM, Kim HK, Shim W, Anwar MA, Kwon JW, Kwon HK *et al.* Mechanism of Cisplatin-Induced Cytotoxicity Is Correlated to Impaired Metabolism Due to Mitochondrial ROS Generation. *PLoS One* 2015; 10: e0135083.
- 6 Chou TC, Talalay P. Quantitative analysis of dose-effect relationships: the combined effects of multiple drugs or enzyme inhibitors. *Adv Enzyme Regul* 1984; 22: 27-55.
- 7 Dasari S, Tchounwou PB. Cisplatin in cancer therapy: molecular mechanisms of action. *Eur J Pharmacol* 2014; 740: 364-378.
- 8 Di Veroli GY, Fornari C, Wang D, Mollard S, Bramhall JL, Richards FM *et al.* Combenefit: an interactive platform for the analysis and visualization of drug combinations. *Bioinformatics* 2016; 32: 2866-2868.
- 9 Ernst M, Putoczki TL. Molecular pathways: IL11 as a tumor-promoting cytokine-translational implications for cancers. *Clin Cancer Res* 2014; 20: 5579-5588.
- 10 Galluzzi L, Senovilla L, Vitale I, Michels J, Martins I, Kepp O *et al.* Molecular mechanisms of cisplatin resistance. *Oncogene* 2012; 31: 1869-1883.

- 11 Hanker LC, Loibl S, Burchardi N, Pfisterer J, Meier W, Pujade-Lauraine E *et al.* The impact of second to sixth line therapy on survival of relapsed ovarian cancer after primary taxane/platinum-based therapy. *Ann Oncol* 2012; 23: 2605-2612.
- 12 James C, Ugo V, Le Couedic JP, Staerk J, Delhommeau F, Lacout C *et al.* A unique clonal JAK2 mutation leading to constitutive signalling causes polycythaemia vera. *Nature* 2005; 434: 1144-1148.
- 13 Jazaeri AA, Shibata E, Park J, Bryant JL, Conaway MR, Modesitt SC *et al.* Overcoming platinum resistance in preclinical models of ovarian cancer using the neddylation inhibitor MLN4924. *Mol Cancer Ther* 2013; 12: 1958-1967.
- 14 Kang MA, So EY, Simons AL, Spitz DR, Ouchi T. DNA damage induces reactive oxygen species generation through the H2AX-Nox1/Rac1 pathway. *Cell Death Dis* 2012; 3: e249.
- 15 Kelland L. The resurgence of platinum-based cancer chemotherapy. *Nat Rev Cancer* 2007; 7: 573-584.
- 16 Klampfl T, Gisslinger H, Harutyunyan AS, Nivarthi H, Rumi E, Milosevic JD *et al.* Somatic mutations of calreticulin in myeloproliferative neoplasms. *N Engl J Med* 2013; 369: 2379-2390.
- 17 Langdon SP, Lawrie SS, Hay FG, Hawkes MM, McDonald A, Hayward IP *et al.* Characterization and properties of nine human ovarian adenocarcinoma cell lines. *Cancer Res* 1988; 48: 6166-6172.
- 18 Levine RL, Wadleigh M, Cools J, Ebert BL, Wernig G, Huntly BJ *et al.* Activating mutation in the tyrosine kinase JAK2 in polycythemia vera, essential thrombocythemia, and myeloid metaplasia with myelofibrosis. *Cancer Cell* 2005; 7: 387-397.
- 19 Ma L, Clayton JR, Walgren RA, Zhao B, Evans RJ, Smith MC *et al.* Discovery and characterization of LY2784544, a small-molecule tyrosine kinase inhibitor of JAK2V617F. *Blood Cancer J* 2013; 3: e109.
- 20 Marullo R, Werner E, Degtyareva N, Moore B, Altavilla G, Ramalingam SS *et al.* Cisplatin induces a mitochondrial-ROS response that contributes to cytotoxicity depending on mitochondrial redox status and bioenergetic functions. *PLoS One* 2013; 8: e81162.
- 21 McGuire WP, Hoskins WJ, Brady MF, Kucera PR, Partridge EE, Look KY *et al.* Cyclophosphamide and cisplatin compared with paclitaxel and cisplatin in patients with stage III and stage IV ovarian cancer. *N Engl J Med* 1996; 334: 1-6.
- 22 Nangalia J, Massie CE, Baxter EJ, Nice FL, Gundem G, Wedge DC *et al.* Somatic CALR mutations in myeloproliferative neoplasms with nonmutated JAK2. *N Engl J Med* 2013; 369: 2391-2405.

- 23 Olive PL, Banath JP. The comet assay: a method to measure DNA damage in individual cells. *Nat Protoc* 2006; 1: 23-29.
- 24 Onnis B, Fer N, Rapisarda A, Perez VS, Melillo G. Autocrine production of IL-11 mediates tumorigenicity in hypoxic cancer cells. *J Clin Invest* 2013; 123: 1615-1629.
- 25 Ozols RF, Bundy BN, Greer BE, Fowler JM, Clarke-Pearson D, Burger RA *et al.* Phase III trial of carboplatin and paclitaxel compared with cisplatin and paclitaxel in patients with optimally resected stage III ovarian cancer: a Gynecologic Oncology Group study. *J Clin Oncol* 2003; 21: 3194-3200.
- 26 Parganas E, Wang D, Stravopodis D, Topham DJ, Marine JC, Teglund S *et al.* Jak2 is essential for signaling through a variety of cytokine receptors. *Cell* 1998; 93: 385-395.
- 27 Park CY, Krishnan A, Zhu Q, Wong AK, Lee YS, Troyanskaya OG. Tissue-aware data integration approach for the inference of pathway interactions in metazoan organisms. *Bioinformatics* 2015; 31: 1093-1101.
- 28 Quintas-Cardama A, Kantarjian H, Cortes J, Verstovsek S. Janus kinase inhibitors for the treatment of myeloproliferative neoplasias and beyond. *Nat Rev Drug Discov* 2011; 10: 127-140.
- 29 Quintas-Cardama A, Verstovsek S. Molecular pathways: Jak/STAT pathway: mutations, inhibitors, and resistance. *Clin Cancer Res* 2013; 19: 1933-1940.
- 30 Scott LM, Tong W, Levine RL, Scott MA, Beer PA, Stratton MR *et al.* JAK2 exon 12 mutations in polycythemia vera and idiopathic erythrocytosis. *N Engl J Med* 2007; 356: 459-468.
- 31 Siegel RL, Miller KD, Jemal A. Cancer Statistics, 2017. *CA Cancer J Clin* 2017; 67: 7-30.
- 32 Szasz AM, Lanczky A, Nagy A, Forster S, Hark K, Green JE *et al.* Cross-validation of survival associated biomarkers in gastric cancer using transcriptomic data of 1,065 patients. *Oncotarget* 2016; 7: 49322-49333.
- 33 Tasdogan A, Kumar S, Allies G, Bausinger J, Beckel F, Hofemeister H *et al.* DNA Damage-Induced HSPC Malfunction Depends on ROS Accumulation Downstream of IFN-1 Signaling and Bid Mobilization. *Cell Stem Cell* 2016; 19: 752-767.
- 34 Trachootham D, Alexandre J, Huang P. Targeting cancer cells by ROS-mediated mechanisms: a radical therapeutic approach? *Nat Rev Drug Discov* 2009; 8: 579-591.

- 35 Tyner JW, Bumm TG, Deininger J, Wood L, Aichberger KJ, Loriaux MM *et al.* CYT387, a novel JAK2 inhibitor, induces hematologic responses and normalizes inflammatory cytokines in murine myeloproliferative neoplasms. *Blood* 2010; 115: 5232-5240.
- 36 Wang D, Lippard SJ. Cellular processing of platinum anticancer drugs. *Nat Rev Drug Discov* 2005; 4: 307-320.
- 37 Wu SC, Li LS, Kopp N, Montero J, Chapuy B, Yoda A *et al.* Activity of the Type II JAK2 Inhibitor CHZ868 in B Cell Acute Lymphoblastic Leukemia. *Cancer Cell* 2015; 28: 29-41.
- 38 Yu X, Vazquez A, Levine AJ, Carpizo DR. Allele-specific p53 mutant reactivation. *Cancer Cell* 2012; 21: 614-625.

Figure legends

Figure 1. Identification of LY2784544 that re-sensitize platinum-resistant ovarian cancer cells to platinum drugs by qHTCS

(A) Schematics illustration of the combination of qHTCS and genomic sequencing for the identification of potent compounds to overcome platinum resistant as well as for the identification of novel cisplatin resistant mechanisms. Alphabetical letters indicate potential targeting pathways.

(B) Viability of SKOV3 and SKOV3 CR cells (left), IGROV1 and IGROV1 CR (right) treated with increasing concentrations of cisplatin for 5 days. The IC₅₀ was indicated.

(C) Heatmap: enrichment of SKOV3 CR for a strong response to specific drug categories (rows) combine with cisplatin. Drug-category-response scores are based on IC₅₀ (μM). The three compounds with reciprocal synergy with cisplatin are indicated.

(D) Synergy matrix (bottom) and surface plots (top) showing the synergy between cisplatin and LY2784544 in SKOV3 and SKOV3 CR cells (n = 3).

(E) The synergistic effects of LY2784544 and cisplatin on IGROV1 CR cells. CI values are presented below the bars.

(F) Viability of PEO1 and PEO4 cells treated with increasing concentrations of cisplatin for 5 days. The IC₅₀ was indicated.

(G) The synergistic effects of LY2784544 and cisplatin on PEO4 cells. The CI values are presented below the bars.

In all panels of this figure, data are represented as mean ± SD from three independent experiments performed in triplicate.

Figure 2. LY2784544 targets JAK2 signaling in platinum resistant ovarian cancer cell *in vitro* and *in vivo*

(A) Phosphorylation of JAK2 and STAT5 in parental and platinum resistant ovarian cancer cells.

(B) JAK2 knockdown by shRNA decreases phosphorylation of JAK2 and STAT5 in puromycin-selected SKOV3 CR cells.

(C) Viability of SKOV3 CR cells treated with increasing concentrations of cisplatin for 5 days after JAK2 knockdown. Data are represented as mean \pm SD from three independent experiments performed in triplicate. *** $p < 0.001$ by two-way ANOVA.

(D) LY2784544 down-regulates JAK2-STAT5 signaling in SKOV3 CR cells. Cells were treated with the indicated concentrations of LY2784544 for 48 hr.

(E) Immunoblotting for the indicated proteins in SKOV3 CR cells treated with vehicle, 3 μ M LY2784544, 5 μ M cisplatin, or the combination (Combo) for 48 hr.

(F) Apoptosis percentage of SKOV3 CR cells treated with vehicle, 3 μ M LY2784544, 5 μ M cisplatin, or the combination (Combo) for 48 hr and analyzed for Annexin V and Propidium Iodide staining by flow cytometry. Data are represented as mean \pm SD from three independent experiments performed in triplicate. ** $p < 0.01$, *** $p < 0.001$, n.s. means not significant by one-way ANOVA.

(G) Growth curves of SKOV3 CR xenograft tumors treated with vehicle, LY2784544 (15 mg/kg/day intraperitoneally), cisplatin (8 mg/kg/week intraperitoneally), or LY2784544 plus cisplatin (Combo) for 2 weeks. Data are represented as means \pm SEM, $n = 6$ mice/group. *** $p < 0.001$ by two-way ANOVA. A photograph of the representative tumor from mice in each treatment arm is shown. Ruler scale is in cm.

(H) Kaplan-Meier survival curves of SKOV3 CR tumor-bearing mice treated with cisplatin and/or LY2784544 as in (G). The endpoint was scored when a tumor reached 1.5 cm or when a mouse showed any sign of distress. ($n = 6$, * $p < 0.05$, ** $p < 0.01$ by log-rank (Mantel-Cox) test).

(I) Representative hematoxylin and eosin (H&E), IHC and TUNEL staining of tumor samples from mice treated with cisplatin and/or LY2784544, tumors were collected 4 days after the last treatment. Scale bar, 100 μ m for H&E and pJAK2 IHC, 50 μ m for TUNEL.

(J) Quantification of IHC staining for pJAK2 in tumors treated as in (I). $n = 5$ mice/group. Data are represented as means \pm SEM. * $p < 0.05$, ** $p < 0.01$, *** $p < 0.001$, n.s. means not significant by one-way ANOVA.

(K) Quantification of apoptotic cells in tumors treated as in (I). Data are represented as mean \pm SD. $n = 5$ mice/group. *** $p < 0.001$, n.s. means not significant by one-way ANOVA.

Figure. 3. IL-11 regulates JAK2 activity and cisplatin resistance in ovarian cancer cells

(A) Viability of SKOV3 cells treated with increasing concentrations of cisplatin for 5 days after pretreatment for 2 days with the indicated amount of conditioned medium from SKOV3 or SKOV3 CR cells. Data are represented as mean \pm SD from three independent experiments performed in triplicate. CM, conditioned medium. * $p < 0.05$, ** $p < 0.01$, *** $p < 0.001$ by Student's t-test.

(B) Phosphorylation of JAK2 and STAT5 in SKOV3 cells after pretreatment for 2 days with the indicated amount of conditioned medium from SKOV3 or SKOV3 CR cells. CM, conditioned medium.

(C and D) Representative image (C) and quantification (D) of cytokine arrays of the expression levels of the indicated cytokines detected in the culture medium of paired cisplatin-sensitive (SKOV3, PEO1) and resistant (SKOV3 CR, PEO4) ovarian cancer cells. Data are represented as mean \pm SD. Numbers above the symbols show the fold change of cytokines in paired cisplatin-sensitive and resistant ovarian cancer cells.

(E) Volcano plot showing up-regulated and down-regulated genes in SKOV3 CR compared with SKOV3. A change is considered significantly if the p -value is < 0.05 and the change is > 2 -fold. Genes with very significant p -values are shown in the figure with p -value= 1×10^{-5} . The bright area in the plot indicates the high density of genes.

(F) Hierarchical clustering of selected cytokine genes reveals a significant 2-fold change in SKOV3 CR compared with SKOV3. Colors in the heatmap represent the gene expression levels after z-score normalization across different samples.

(G) Venn diagram shows the overlap of genes in the KEGG JAK/STAT signaling pathway (Pathway: map04630), genes identified by genomic sequencing of SKOV3/SKOV3 CR cells and genes identified by the cytokine array.

(H and I) Bar graphs showing the levels of mRNA (h) and secreted IL-11 (i) and in ovarian cancer parental cells (SKOV3, IGROV1, PEO1) and cisplatin resistant cells (SKOV3 CR, IGROV1 CR, PEO4). Levels of *IL-11* mRNA and IL-11 protein were measured by RT-qPCR and ELISA respectively and are shown as means \pm SD from three independent experiments performed in triplicate. ** $p < 0.01$ by Student's t-test.

Figure 4. IL-11-mediated autocrine mechanism promotes cisplatin resistance via regulating JAK2-STAT5 activation in ovarian cancer cells

(A) Immunoblotting of phosphorylated JAK2 and STAT5 in SKOV3 cells treated with 10 ng/mL of IL-11 for 4 hr.

(B) Viability of SKOV3 cells incubated with 10 ng/mL of IL-11 for 4hr and then treated with increasing concentrations of cisplatin for 5 days. Data are represented as mean \pm SD from three independent experiments performed in triplicate. ** $p < 0.01$, *** $p < 0.001$ by Student's t-test.

(C) Immunoblotting of phosphorylated JAK2 and STAT5 in SKOV3 CR and IGROV1 CR cells treated with control mouse IgG or neutralizing anti-IL-11 antibody for 4 hr.

(D) Viability of SKOV3 CR (top) and IGROV1 CR (bottom) cells incubated with a control mouse IgG or an IL-11 neutralizing antibody for 4 hr and then treated with increasing concentrations of cisplatin for 5 days. Data are represented as mean \pm SD from three independent experiments performed in triplicate. ** $p < 0.01$, *** $p < 0.001$ by Student's t-test.

(E) The levels of IL-11 secretion in SKOV3 CR cells transfected with IL11 shRNA and selected with puromycin. *** $p < 0.001$ by one-way ANOVA.

(F) Immunoblotting of phosphorylated JAK2 and STAT5 in SKOV3 CR cells transfected with IL11 shRNA and selected with puromycin.

(G) Viability of SKOV3 CR cells treated with increasing concentrations of cisplatin for 5 days after IL-11 knockdown with IL11 shRNA. Data are represented as mean \pm SD from three independent experiments performed in triplicate. *** $p < 0.001$ by two-way ANOVA.

(H) Recombinant IL-11 reversed the effect of IL11 shRNA on the sensitivity of SKOV3 CR cells to cisplatin. SKOV3 CR shIL-11 cells were incubated with IL-11 (17 pg/ml for SKOV3 CR shIL11-1; 47 pg/ml for SKOV3 CR shIL11-2; calculated from 5e) for 4 hr and then treated with 1 μ M of cisplatin for 5 days. Data are represented as mean \pm SD from three independent experiments performed in triplicate. ** $p < 0.01$, *** $p < 0.001$ by one-way ANOVA.

(I) Knockdown JAK2 by siRNA block IL-11 mediated resistance of SKOV3 cells to cisplatin. SKOV3 cells were transfected with JAK2 siRNA for 24hr and then incubated with recombinant IL-11 for 4 hr, followed by increasing concentrations of cisplatin treatment for 5 days. *** $p < 0.001$ by two-way ANOVA.

Figure 5. Cisplatin treatment induces IL-11 secretion and JAK2-STAT5 activation *in vitro* and *in vivo*

(A) IL-11 levels measured by ELISA in the medium of SKOV3 cells treated with cisplatin of various dosages for 4 days (left) and 1 μ M for various times (right) as indicated. Data are represented as mean \pm SD from three independent experiments performed in triplicate. ** $p < 0.01$, *** $p < 0.001$ by one-way ANOVA.

(B) *IL11* mRNA were measured by qPCR in SKOV3 cells treated with cisplatin of various dosages for 4 days (left) and 1 μ M for various times (right) as indicated. Data are represented as mean \pm SD from three independent experiments performed in triplicate. ** $p < 0.01$, *** $p < 0.001$ by one-way ANOVA.

(C) Levels of phosphorylated JAK2 and STAT5 in SKOV3 cells treated with cisplatin of various dosages for 4 days (left) and 1 μ M for various times (right) as indicated.

(D) A schematic presentation of the experimental set-up.

(E) Serum IL-11 levels measured by ELISA in mice bearing SKOV3 xenograft tumors and treated with vehicle or cisplatin (2 - 6 mg/kg/twice a week intraperitoneally for 2 weeks) as in (D). Data are represented as mean \pm SD. $n = 3$ mice/group. *** $p < 0.001$ by one-way ANOVA.

(F) Representative H&E and IHC images of SKOV3 xenograft tumors treated as in (D).

(G) Quantification of IHC staining for pJAK2 and IL-11 in tumors as in (F). Data are represented as means \pm SEM. * $p < 0.05$, ** $p < 0.01$, *** $p < 0.001$, n.s. means not significant by one-way ANOVA.

Figure 6. ROS induces IL-11 expression by promoting expression of *FOSL1* (FRA1)

(A) Representative images (left) and quantification (right) of reactive oxygen species (ROS) production in SKOV3 and SKOV3 CR cells. Data are represented as means \pm SD from three independent experiments. ** $p < 0.01$ by Student's t-test. Scale bar, 100 μ m.

(B) Quantification of reactive oxygen species (ROS) production in SKOV3 CR cells after treated with the ROS inhibitor YCG063 20 μ M for 24 hr. Data are represented as means \pm SD from three independent experiments. *** $p < 0.001$ by Student's t-test.

(C) IL-11 levels measured by ELISA in the medium of SKOV3 CR cells treated with YCG063 20 μ M for 24 hr. Data are represented as mean \pm SD from three independent experiments performed in triplicate. *** $p < 0.001$ by Student's t-test.

(D) Immunoblotting of phosphorylated JAK2 and STAT5 in SKOV3 CR cells treated with YCG063 (20 μ M) for 24 hr.

(E) Quantification of reactive oxygen species (ROS) production in SKOV3 cells after treated with the ROS inhibitor YCG063 (20 μ M), cisplatin (1 μ M), or both for 24 hr. Data are represented as means \pm SD from three independent experiments. ** $p < 0.01$, *** $p < 0.001$, n.s. means not significant by one-way ANOVA.

(F) IL-11 levels measured by ELISA in SKOV3 cells treated with YCG063 (20 μ M), cisplatin (1 μ M) or both for 24 hr. Data are represented as mean \pm SD from three independent experiments performed in triplicate. *** $p < 0.001$ by one-way ANOVA.

(G) Immunoblotting of phosphorylated JAK2 and STAT5 in SKOV3 CR cells treated with YCG063 (20 μ M), cisplatin (1 μ M) or both for 24 hr.

(H) Heatmap of transcription factors that can potentially regulate *IL11* in SKOV3 and SKOV3 CR. Colors in the heat-map represent the gene expression levels after z-score normalization across different samples. Fold change bar on the right shows that *FOSL1* is the most significant up-regulated gene.

(I) Total and phosphorylated levels of FRA1 in SKOV3 and SKOV3 CR cells.

(J) Depletion of *FOSL1* by siRNA decreases the phosphorylated and total FRA1 protein levels in SKOV3 CR cells

(K) IL-11 levels measured by ELISA in the medium of SKOV3 CR cells transfected with *FOSL1* siRNA for 48 hr. Data are represented as mean \pm SD from three independent experiments performed in triplicate. *** $p < 0.001$ by Student's t-test.

(L) Immunoblotting of phosphorylated and total FRA1 protein in SKOV3 CR cells treated with YCG063 20 μ M for 24 hr.

Figure 7. Clinical evidence of activated IL-11-JAK2 pathway in platinum drug resistant ovarian cancer patients

(A) Comparison of the mRNA IL-11 levels measured by qPCR in platinum sensitive (n = 23) and resistant (n = 16) ovarian cancer patients. * $p < 0.05$ by unpaired student t-test. Sen, sensitive cases. Res, resistant cases.

(B) Comparison of the serum IL-11 levels measured by ELISA in platinum sensitive (n = 21) and resistant (n = 16) ovarian cancer patients. **p < 0.01 by unpaired student t-test. Sen, sensitive cases. Res, resistant cases.

(C) Kaplan–Meier survival curves showing 5-year PFS rate (left panel) and OS rate (right panel) of 37 ovarian cancer patients as shown in (d), who were stratified by serum IL-11 levels (40 pg/ml); log-rank (Mantel-Cox), *P* values and HRs are shown.

(D) Representative IHC image (left panel) and quantification (right panel) of the cisplatin sensitive and resistant tumor samples from the same patient (P1).

(E) IHC quantification of IL-11 and p-JAK2 in platinum sensitive and recurrent tumor samples from seven patients (P2-P8). Data are represented as mean ± SD.

(F) Scatter plots showing a correlation between IL-11 and pJAK2 levels in both primary and recurrent patient tumors (P2-P8).

(G) Venn diagram indicating the overlap of genes in the JAK2 functional gene set and up-regulated genes set in SKOV3 CR compared with that in SKOV3 cells (left panel). The heatmap (right panel) shows 22 overlapped genes (JAK signature gene set). Colors in the heatmap represent the gene expression levels after z-score normalization across different samples.

(H) Kaplan–Meier analyses of 5-year PFS rate (left panel) and OS rates (right panel) based on clinical and molecular data for ovarian cancer patients (n = 502 for PFS, n = 478 for OS). The patients were stratified by the expression levels in their tumors of the JAK2 signature genes. Medium survival, log-rank (Mantel-Cox) p values and HRs are shown.

Figure 2

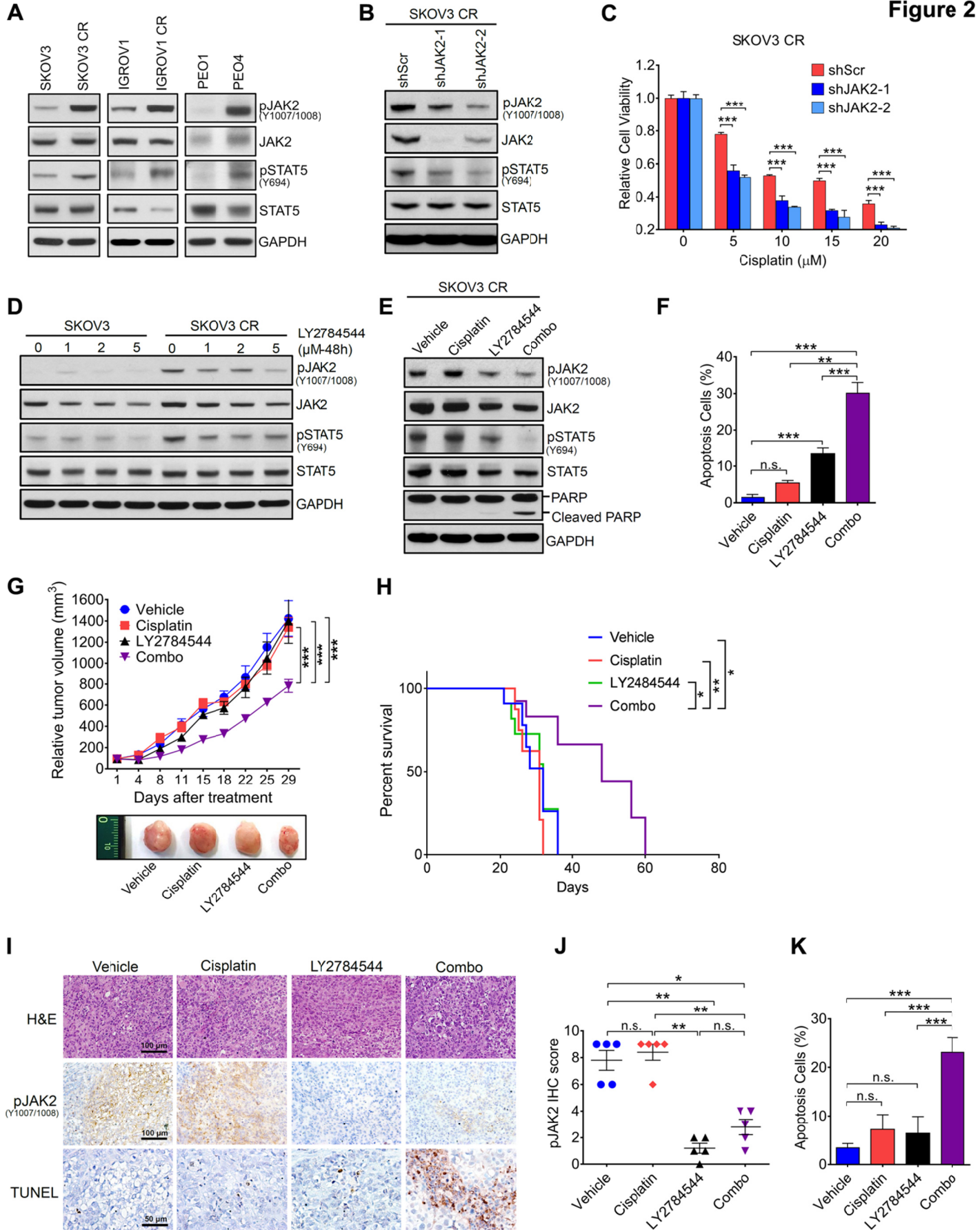


Figure 3

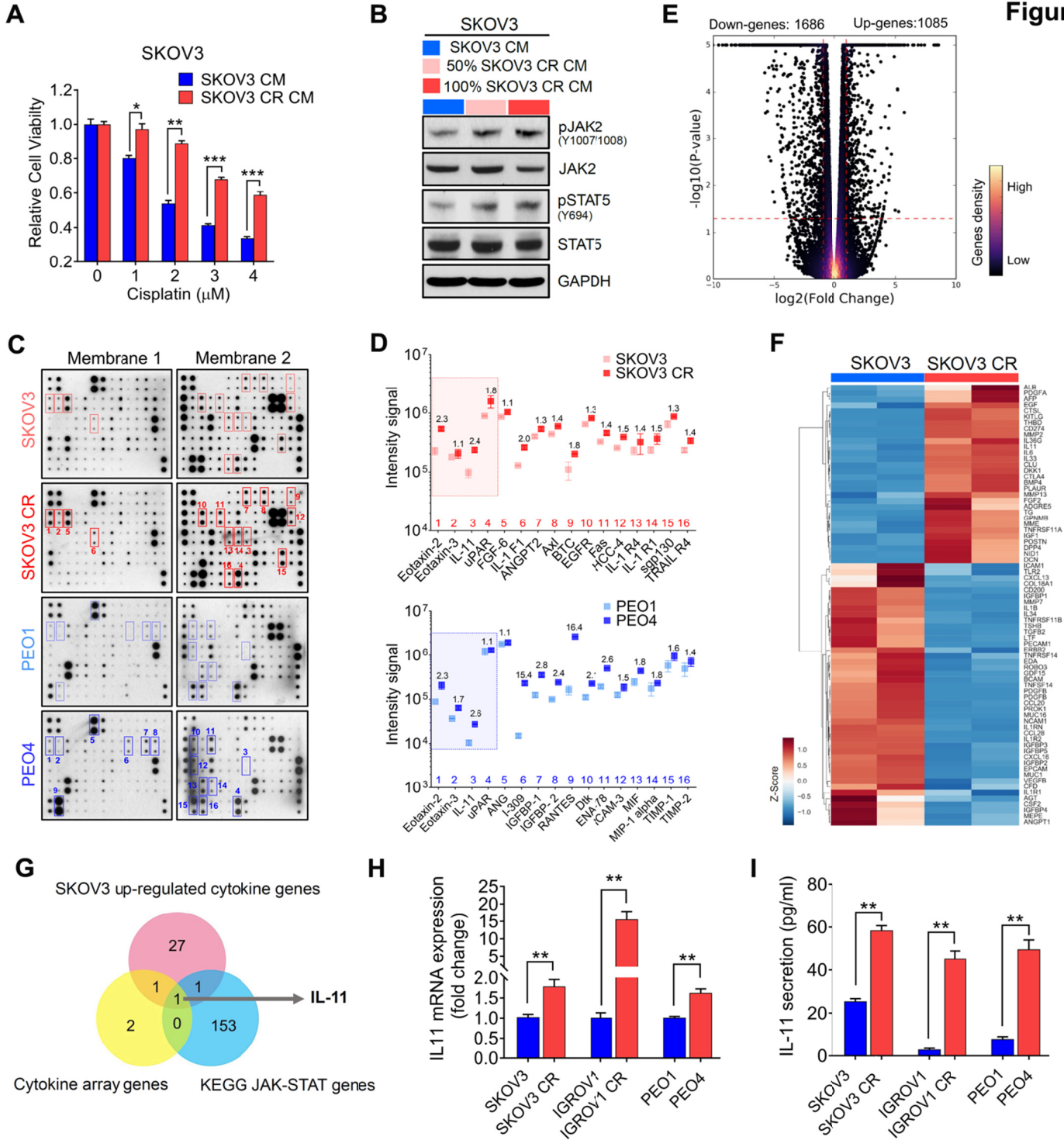
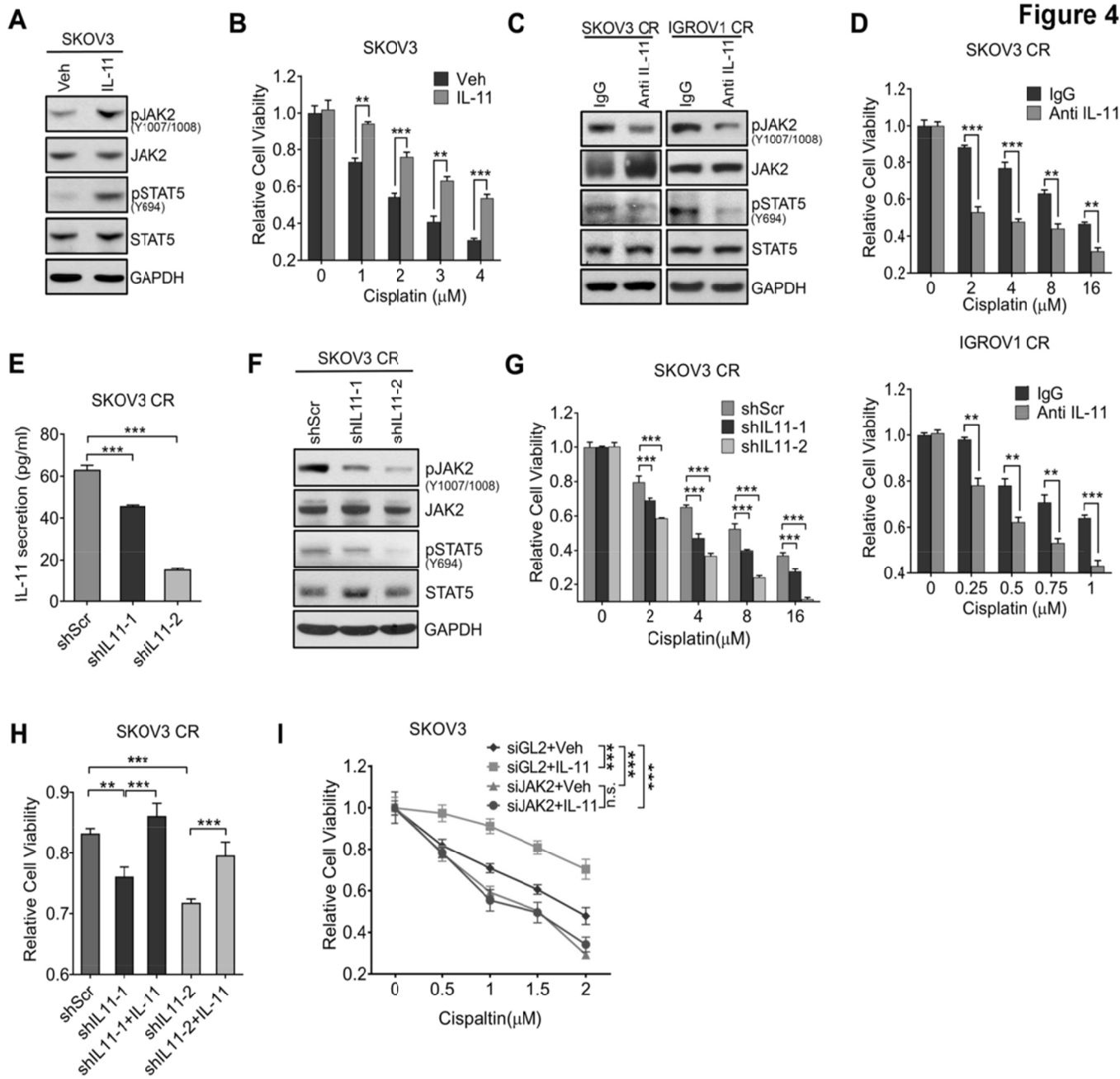


Figure 4



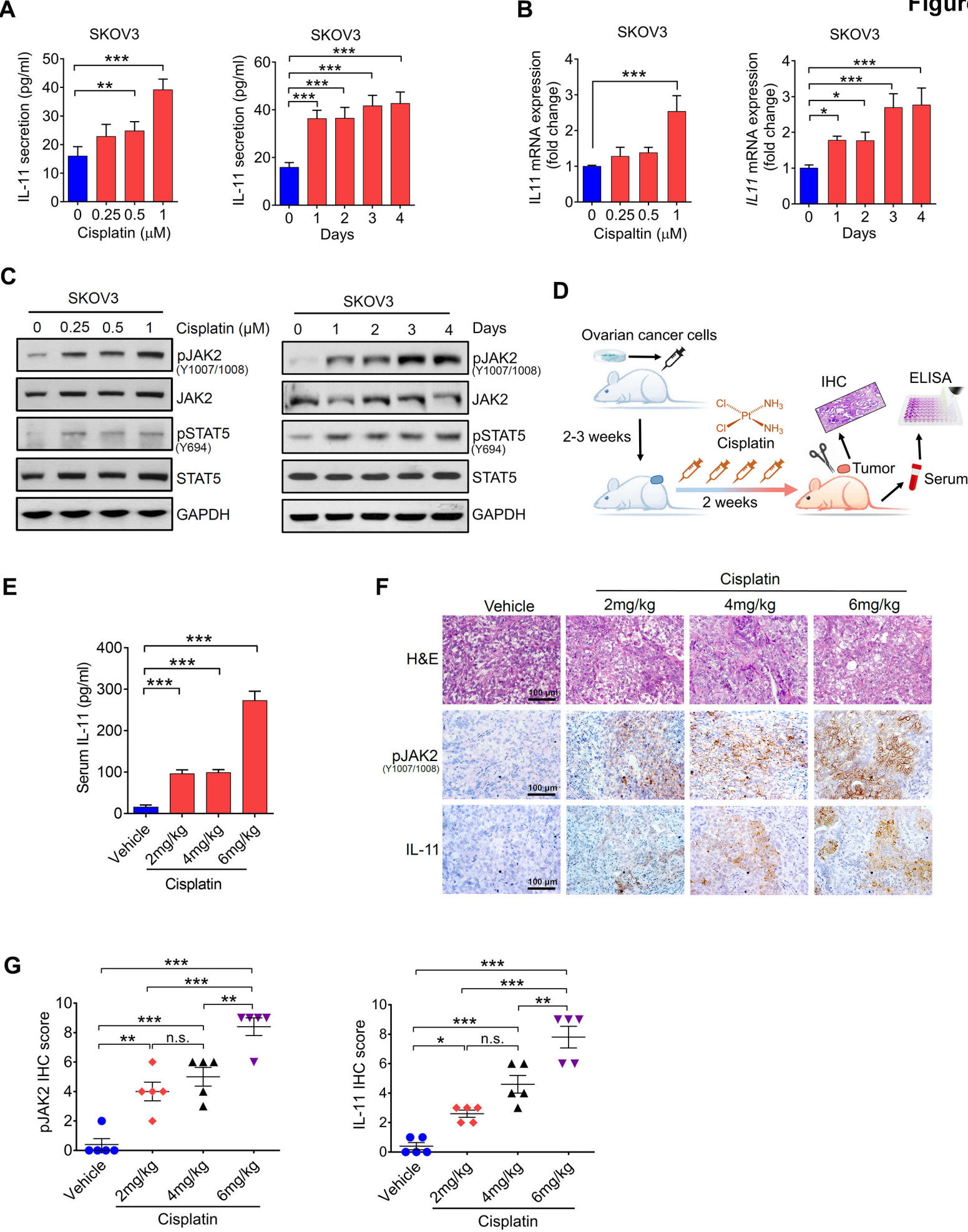


Figure 6

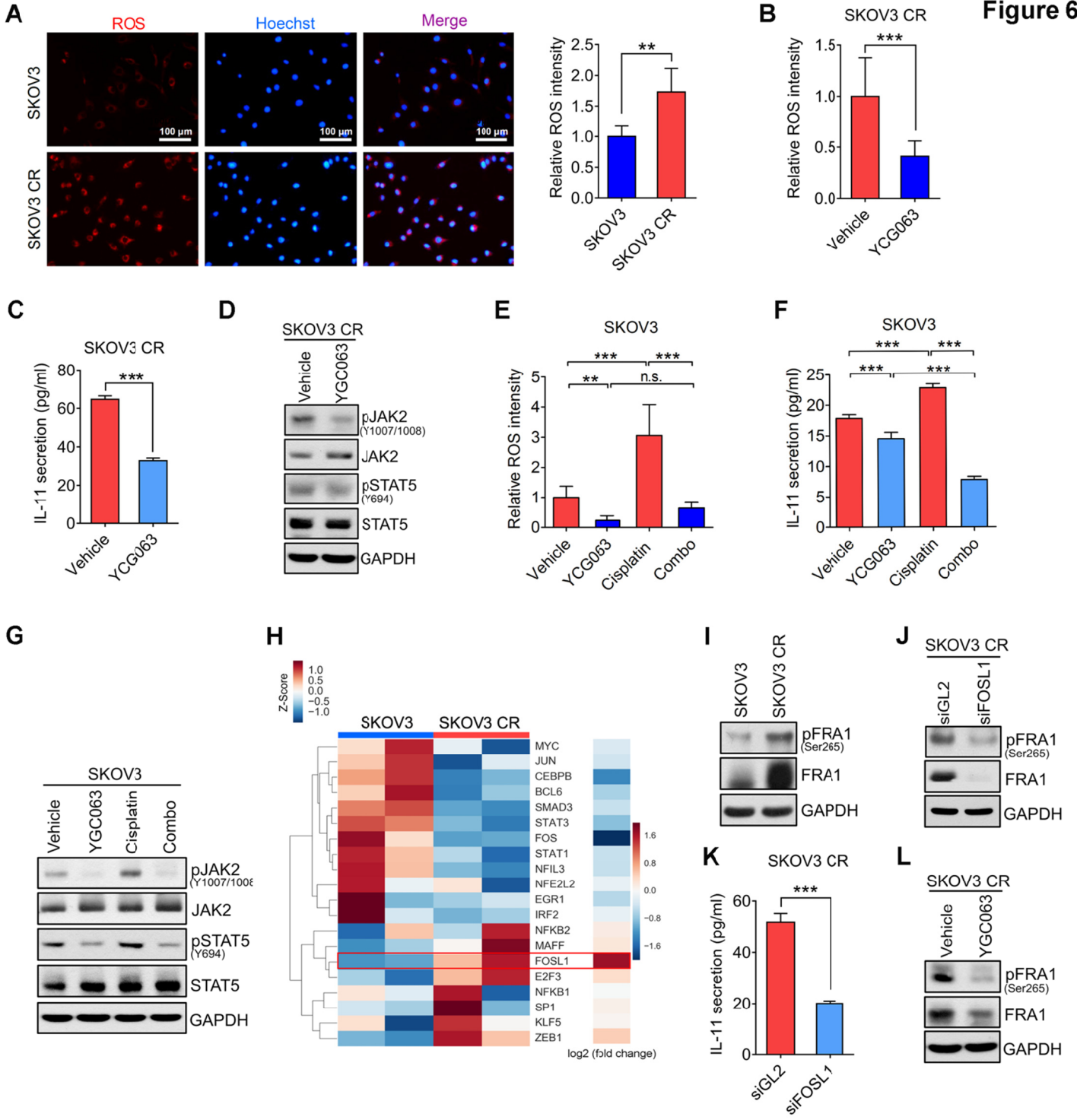


Figure 7

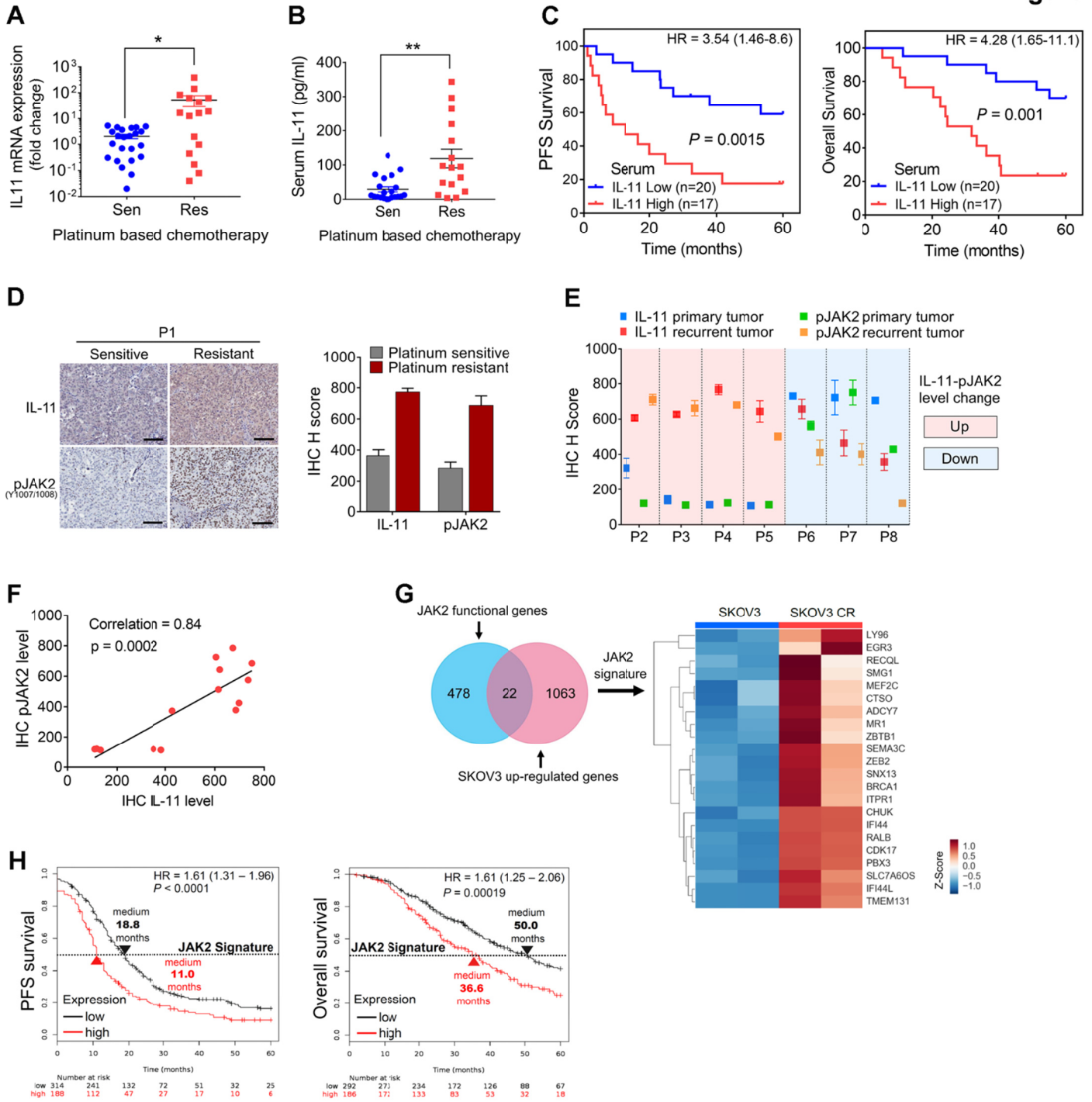


Table and their legends

Table S1. Compounds of secondary hits by qHTCS

Table S2. Correlation between patient serum IL-11 level and clinical characteristics of HKU qPCR set

Table S3. Correlation between patient serum IL-11 level and clinical characteristics of HKU ELISA set.

Table S4. Patient characteristics of HKU IHC set.

Table S1. Compounds of secondary hits by qHTCS

Sample Name	Primary MOA	Diff AUC	Diff IC ₅₀ (μ M)	Vehicle		20 μ M Cisplatin	
				IC ₅₀ (μ M)	AUC	IC ₅₀ (μ M)	AUC
Ingenol mebutate	PKC Activator	112.60	7352.94	null	0.00	0.01	112.60
LY2784544	Jak2 inhibitor	9.36	31.63	8.56	74.73	0.27	84.09
GSK-2636771	PI3Kbeta inhibitor	47.17	19.95	27.06	39.73	1.36	86.91
Delanzomib	Proteasome Inhibitor	29.49	19.95	3.41	102.73	0.17	132.22
Bortezomib	Proteasome Inhibitor	10.16	5.01	0.34	138.79	0.07	148.95
Marizomib	Proteasome Inhibitor	7.80	2.51	0.14	165.67	0.05	173.47
MLN-4924	NEDD8-Activating Enzyme (NAE) Inhibitors	131.54	1.58	1.71	6.19	1.08	137.73
Digoxin	Steroid	65.87	0.79	0.11	99.52	0.14	165.40
Ouabain octahydrate	null	54.35	0.79	0.11	100.19	0.14	154.54
Triptolide	Inhibition of RNA polymerase II mediated transcription	75.31	0.63	0.01	1.53	0.02	76.84
G-Strophanthin	Na ⁺ /K ⁺ -ATPase Inhibitors	89.18	0.63	0.07	83.23	0.11	172.42
NSC319726	Mutant p53 Activator	63.60	0.50	0.04	33.55	0.09	97.15
Thapsigargin	PKC Activator	92.02	0.40	0.01	24.37	0.03	116.39

MOA, mechanism of action; Diff, difference; AUC, area under the curve.

Table S2. Correlation between patient serum IL-11 level and clinical characteristics of HKU qPCR set

Characteristics	Total	mRNA IL-11 Level		OR	95% CI	P-value
		Low	High			
All Cases	39	20 (51.3%)	19 (48.7%)			
Age (years)						
≥50	15	6 (40.0%)	9 (60.0%)			
<50	22	14 (63.6%)	8 (36.3%)	0.381	0.11-1.49	0.156
Stage						
I	10	6 (60.0%)	4 (40.0%)			
II	5	2 (40.0%)	3 (60.0%)			
III	17	7 (41.2%)	10 (58.8%)			
IV	7	5 (71.4%)	2 (28.6%)			0.495
Histological type						
Serous	17	10 (58.8%)	7 (41.2%)			
Nonserous	232	10 (45.5%)	12 (54.5%)	1.714	0.49-6.20	0.408
Grade						
1	7	4 (57.1%)	3 (42.9%)			
2	10	5 (50.0%)	5 (50.0%)			
3	22	11 (50.0%)	11 (50.0%)			0.943

PFS, progressive free survival; OS, overall survival.

P-value calculated by Chi-square test.

Table S3. Correlation between patient serum IL-11 level and clinical characteristics of HKU ELISA set

Characteristics	Total	Serum IL-11 Level		OR	95% CI	P-value
		<40 pg/ml	≥40 pg/ml			
All Cases	37	20 (54.1%)	17 (45.9%)			
Age (years)						
≥50	22	14 (63.6%)	8 (36.4%)			
<50	15	6 (40.0%)	9 (60.0%)	2.625	0.67-9.29	0.156
Stage						
I	7	5 (71.4%)	2 (28.6%)			
II	2	2 (100%)	0 (0%)			
III	21	10 (47.6%)	11 (52.4%)			
IV	7	3 (42.9%)	4 (57.1%)			0.354
Histological type						
Serous	14	8 (57.1%)	6 (42.9%)			
Nonserous	23	12 (52.2%)	11 (47.8%)	1.222	0.31-4.12	0.769
Grade						
1	4	3 (75%)	1 (25%)			
2	12	8 (66.7%)	4 (33.3%)			
3	21	9 (42.9%)	12 (57.1%)			0.282

PFS, progressive free survival; OS, overall survival.

P-value calculated by Chi-square test.

Table S4. Patient characteristics of HKU IHC set

Patient	Age (years)	Stage	Histology	Grade	Chemotherapy	PFS after chemo (months)
1	54	IIIC	Mucinous	2	Carboplatin + Taxol	11
2	58	IC	Clear cell	3	Carboplatin + Taxol	41
3	50	IIC	Endometrioid	3	Carboplatin + Taxol	34
4	68	IIIC	Serous	N/A	Carboplatin + Taxol	25
5	56	IC	Clear cell	1	Carboplatin + Taxol+ Bevacizumab	30
6	78	IC	Serous	3	Carboplatin	22
7	55	IIIC	Clear cell	3	Carboplatin + Taxol	47
8	38	IIIC	Serous	3	Carboplatin + Taxol+ Bevacizumab	18

Supplementary Materials

Autocrine activation of JAK2 BY IL-11 promotes platinum drug resistance

Wei Zhou, Wei Sun, Mingo MH Yung, Sheng Dai, Yihua Cai, Chi-Wei Chen, Yunxiao Meng, Jennifer B Lee, John C Braisted, Yinghua Xu, Noel T Southall, Paul Shinn, Xuefeng Huang, Zhangfa Song, Xiulei Chen, Yan Kai, Xin Cai, Zongzhu Li, Qiang Hao, Annie NY Cheung, Hextan YS Ngan, Stephanie S Liu, Stephanie Barak, Jing Hao, Zhijun Dai, Alexandros Tzatsos, Weiqun Peng, Huadong Pei, Zhiyong Han, David W Chan, Wei Zheng , Wenge Zhu

This file includes:

Supplementary Methods

Figure S1. Establishment of platinum resistant ovarian cancer cell lines and identification of compounds that overcome cisplatin resistance.

Figure S2. Identification of LY2784544 that resensitizes platinum drug by qHTCS

Figure S3. LY2784544 synergies with platinum drugs by JAK2 inhibitors

Figure S4. LY2784544 in vitro kinase assay and in vivo toxicity.

Figure S5. JAK2 gene analysis and receptor expression.

Figure S6. Effects on cisplatin-induced IL-11 secretion by ATR inhibitor or ROS inhibitor.

Figure S7. IL-11 and JAK2 pathway in platinum drug resistant ovarian cancer patients

Table S1. Compounds of secondary hits by qHTCS

Table S2. Correlation between patient serum IL-11 level and clinical characteristics of HKU qPCR set

Table S3. Correlation between patient serum IL-11 level and clinical characteristics of HKU ELISA set.

Table S4. Patient characteristics of HKU IHC set.

Supplementary Methods

Antibodies and reagents

The antibodies for western blotting were obtained from the following companies: Cell Signaling Technology (PARP, pJAK2 (Y1007/1008), JAK2, pSTAT5 (Y694), STAT5, pFRA1 (Ser265), FRA1, pChk1 (Ser317) and Chk1); Santa Cruz Biotechnology (Caspase-9, IL-11R α , IL-6R α , EpoR, G-CSFR); Sigma-Aldrich (GAPDH). The antibodies for immunohistochemistry were from Abcam (pJAK2 (Y1007/1008) and IL-11). The antibody for IL-11 neutralization was from R&D systems (IL-11). Cis-Diamineplatinum(II) dichloride (cisplatin), carboplatin, and Solutol HS 15 were purchased from Sigma-Aldrich. LY2784544 and TG101348 were purchased from Selleckchem, TG46 was purchased from SynKinase. Pru, MLN4924 were purchased from Millipore. Recombinant human IL-11 was purchased from R&D systems. YCG 063 was purchased from Calbiochem.

Compound libraries

To identify compounds that can overcome cisplatin resistance, 6016-compounds from the three compound collections were screened. The library of pharmacologically active compounds (LOPAC[®]) of 1280 compounds (1) was purchased from Sigma. The NCGC Pharmaceutical Collection (NPC) of 2816 compounds and mechanism interrogation plate (MIPE) library of 1920 compounds were previously described (2,3). Compounds from all libraries were obtained as powder and dissolved in dimethyl sulfoxide (DMSO). using Prism software (GraphPad).

Quantitative high-throughput combinational screening (qHTCS)

SKOV3 CR were plated at 1,500 cells/well in 5 μ L assay medium (DMEM+10% FBS) in 1536-well polystyrene plates (Greiner Bio-One) and incubated for 16 hr. Cisplatin was freshly prepared in 0.9%

sodium chloride solution. One microliter of cisplatin in assay medium was transferred into each well of the assay plate using Multidrop Combi (Thermo Fisher Scientific) to reach a final concentration of 20 μ M; 23 nL of the second drug in the 1536-well compound plate was transferred into the assay plate using NX-TR pin tool station (WAKO Scientific Solutions). After 72 hr incubation, 4 μ L/well ATP detection solution from an ATP content cell viability assay kit (Promega) was added into the assay plate using Multidrop Combi. Following another 30 mins incubation at room temperature, the luminescence signal was measured using a ViewLux plate reader (PerkinElmer). The primary screen data and curve fitting were analyzed using software developed at the NIH Chemical Genomics Center (NCGC)³⁹. In the qHTCS, the cytotoxic effect of a two-drug combination was compared to that of single drug. Briefly, the first compounds at 11 concentrations were tested with IC20 and IC50 of a second compound or vehicle (control). A heatmap of the drug combinations was constructed where columns enumerate cisplatin/vehicle, rows enumerate the other drug, and heat map elements are IC50. The IC50 values were computed by fitting the concentration response titrations (using the normalized, corrected signal) to the hill equation from which the IC50 values were calculated as the concentration at which the fitted curve reaches 50% of maximum. Half maximal inhibitory concentration (IC50) values were calculated .

Animal experiments

Four to six weeks old female BALB/c athymic nude mice (CByJ.Cg-Foxn1nu/J) were purchased from the Jackson Laboratory. All studies involving mice were carried out in accordance with the National Institutes of Health regulation concerning the care and use of experimental animals and with the approval of the Institutional Animal Care and Use Committees (IACUC) of the George Washington

University. The experiments were approved by the Institutional Animal Care and Use Committees of the George Washington University Protocol A305. To establish the subcutaneous cisplatin sensitive and resistant xenografts. 4×10^6 SKOV3 or SKOV3 CR cells were suspended in 100 μ l PBS and injected into the dorsal flank of each mouse. When the average tumor volume reached 100-150 mm^3 , the mice were randomized into subsequent experiment groups. Cisplatin was given intraperitoneally at 8mg/kg weekly for two weeks, and LY2784544 was given intraperitoneally at 15 mg/kg daily for 2 weeks. Tumors were measured twice per week. The relative tumor volumes were calculated using the formula: $a \times (b^2) / 2$, for which a and b represent the longest and shortest diameters, respectively. For survival studies, animals were sacrificed when tumors reached 1.5 cm^3 or when they showed any signs of distress such breathing disorders, weight loss, or immobility. For serum marker and tumor histology evaluation, blood and tumor samples were obtained from the animals 4 days after the final administration for subsequent evaluation. For single cisplatin treatment using SKOV3 tumors, cisplatin was given intraperitoneally at 2 mg/kg, 4 mg/kg and 6 mg/kg twice a week for two weeks. Serum and tumor were collected 4 days after final administration of the drug.

Flow cytometry

Apoptosis was analyzed by using FITC Annexin-V Apoptosis Detection reagents (BD Pharmingen) according to the manufacturer's instructions. Cells were treated with the testing agents for 48hr and then treated with 0.25% trypsin. We then washed cells with cold PBS twice and re-suspended cells in binding buffer (1×10^6 cells /ml). Next 100 μ l of the cell suspension (1×10^5 cells) was incubated with 5 μ l of Annexin-V FITC and 5 μ l of propidium iodide (PI) for 15 min at room

temperature in the dark. The population of apoptosis cells were analyzed by flow cytometry (BD Biosciences).

Modified comet assay

Modified comet assay was performed as according to the instruction of the CometAssay[®] Kit (Trevigen). In brief, cells were incubated with or without cisplatin for 2 hours. DNA was randomly broken into fragments using irradiation at the dose of 20 Gy. Cells (10 μ L in PBS) were mixed with 100 μ L of 1.2 % low melting point agarose and were plated on CometAssay Kit slides. After cells were lysed, DNA was separated from cells by electrophoresis at 20 voltages and 300 mA for 45 minutes. The tail moment was visualized by staining with 100 μ L of 10000-fold diluted SYBR Geen[®]. I. The tail moments of at least 50 cells of each treatment were analyzed with OpenComet software. The degree of DNA interstrand crosslinking (ICLs) present in a drug-treated sample was determined by comparing the tail moments of the irradiated control according to the formula: percentage of DNA with ICLs = $(1 - (TM_{cispt} - TM_{uc} / TM_{ic} - TM_{uc})) \times 100$ %. TM_{cispt} means the tail moment of the cisplatin-treated irradiated sample, TM_{uc} indicates the tail moment of untreated non-irradiated control, and TM_{ic} is a tail moment of untreated irradiated control.

Clonogenic assay

To determine the capacity of clonogenic survival, cells were plated in 60-mm dishes at a density of 300 cells per dish and cultured overnight. Cells were then treated with the drugs at indicated concentrations. Cells were kept in the incubator for 14 days to allow colony formation. The medium was removed, and cells were fixed and stained with 0.5 % crystal violet. Colonies with >50 cells were counted.

KINOMEscan profiling of LY2784544

The KINOMEscan profiling of the LY2784544 was assessed in competition binding assays, using a panel of 468 recombinant kinases (DiscoverX) as described (4). The binding interactions are reported as “% Ctrl”, where lower numbers indicate stronger interactions. Selectivity score or S-score is a quantitative measure of compound selectivity. It is calculated by dividing the number of kinases that compounds bind to by the total number of distinct kinases tested, excluding mutant variants.

JAK2 coding region sequencing

The mRNAs in SKOV3 and SKVO3 CR cells were extracted using RNA extraction kit (Qiagen) and were further converted into cDNA by reverse transcriptase (Invitrogen). The Jak2 coding region was amplified in five fragments using specific pairs of primers: fragment 1, 5'- AGG CAA CAG GAA CAA GAT GTG AAC-3' and 5'- AAG GAC CAC TTC CAG GTT CTT TTA-3', fragment 2, 5'-CAA AGA TCC AAG ACT ATC ATA TTT T-3' and 5'- TTA TAT TGT CTG AGC GAA CAG TTT C-3', fragment 3, 5'- GAA ACT GTT CGC TCA GAC AAT ATA A-3' and 5'- CTT TGA GAA TCC AGA GCA CTT AGA G-3', fragment 4, 5'- TAA ACC TCT AAG TGC TCT GGA TTC T-3' and 5'- TCT CCA ATT TTA ACT CTG TTC TCG T-3', fragment 5, 5'- AGT ACA CAT CTC AGA TAT GCA AGG G-3' and 5'- GGT CTC AGA ATG AAG GTC ATT TC-3'. All the PCR products were sent to Eurofin for DNA sequencing. The sequences of JAK2 coding region in SKOV3 and SKVO3 CR cells were compared and aligned with each other and with JAK2 sequence obtained from NCBI database (Gene ID: 3717) using M-Coffee alignment(5). The known JAK2 point mutations were also surveyed in SKOV3 and SKVO3 CR cells(6) .

RNA-sequencing analysis

SKOV3 and SKOV3 CR cells growing in log phase were harvested. RNA isolation was completed using the Qiagen miRNeasy Mini Kit, and then RNA samples were converted into cDNA libraries using the Illumina TruSeq Stranded mRNA sample preparation kit (Illumina # RS-122-2103). Read counts of each sample were normalized with DESeq and ran a negative binomial two sample test to find significant genes in higher transcript abundance in either the SKOV3 or SKOV3 CR. The

genes had a false discovery rate (FDR) of < 0.05 . A fold change larger than 2 or smaller than 0.5-fold were considered as differentially expressed genes. RNA sequencing data have been deposited in Gene Expression Omnibus (GEO) under accession number GSE98559.

siRNA interference and shRNA

JAK2 siRNA was purchased from Santa Cruz Biotechnology, *FOSL1* siRNA was purchased from Thermo Fisher Scientific. Control Gl2 (Luciferase) siRNA was as described previously (7). Cells were transfected once with siRNA using Lipofectamine RNAiMAX (Thermo Fisher Scientific) according to the manufacturer's instructions. Cells were treated with the indicated agents for analyses 24 or 48 hr after siRNA transfection. *JAK2* shRNA, *IL11* shRNA, and scramble control shRNA were purchased from OriGene. The lentiviral particles expressing these shRNA were packaged and used to infect cancer cells according to the manufacturer's instructions. Cells were selected in puromycin for two weeks before used for the subsequent experiment.

Immunohistochemistry

Paraffin tissue sections were deparaffinized in xylene and hydrated with ethanol solutions. Antigen-retrieval treatment was performed at 121°C for 5 minutes in 10 mM sodium citrate buffer (pH 6.0). Slides were treated with 3% hydrogen peroxide in methanol solution for 10 minutes to quench endogenous peroxidase activity. Nonspecific bindings were blocked by treating slides with 10% normal goat serum for 30 minutes. Slides were incubated with the primary antibody overnight at 4°C. Second antibody incubation, and DAB staining was using SuperPicture™ Polymer Detection Kit (Thermo Fisher Scientific) according to the manufacturer's instructions. The slides were lightly counterstained with hematoxylin.

For quantification of mouse IHC staining, each tumor sample was assessed in at least five fields at 200× or 400× magnification. Immunoreactivity was evaluated semiquantitatively by staining intensity and proportion. The proportion of staining was scored from 0 to 3 as follows: 3, >50% of cells positive; 2, 10% to 49% of cells positive; 1, <10% of cells positive. Staining intensity was scored from 0 to 3 (0, absent; 1, weak; 2, moderate; 3, intense). The final IHC score for each sample was determined by multiplying the intensity and the proportion of stained cells. The analysis was undertaken blindly without knowledge of treatment variables.

For quantification of patient IHC staining, the following formula was applied to get the H score. H score = $\sum (1 + i) p_i$, in this formula, “i” is the intensity score (0, No staining; 1, Weak cytoplasmic/nuclear; 2, Moderate cytoplasmic; 3, Weak nuclear and cytoplasmic; 4, Moderate nuclear; 5, Strong cytoplasmic; 6, Strong nuclear; 7, Moderate nuclear and cytoplasmic; 8, Strong nuclear and cytoplasmic) and “ p_i ” is the percent of the cells with this intensity. The quantification of IHC staining was scored blindly by three independent observers.

TUNEL assay

The In Situ Cell Death Detection Kit (Roche) was used to detect apoptotic tumor cells *in vivo*. In brief, paraffin tissue sections were deparaffinized in xylene and rehydrated in decreasing concentrations of ethanol. Slides were incubated in 0.1 % Triton X-100 (Sigma-Aldrich) for 8 minutes. After wash with distilled water, slides were incubated in 3% hydrogen peroxide in PBS (pH 7.4) for 5 min. After washing with PBS, the slides were incubated in terminal deoxyribonucleotide transferase (TdT) at 37°C for 60 min. After washing with PBS, slides were incubated with horseradish peroxidase (POD) at 37°C for 30 min. DAB Substrate (Thermo Fisher Scientific) was used to demonstrate peroxidase activity. Slides were counterstained with

hematoxylin before observation. At least 2000 cells were counted under a microscope at 400x magnification in randomly-selected fields to quantify apoptosis.

RT-qPCR

RNA was extracted by using the RNeasy Mini Kit according to the manufacturer's protocol (QIAGEN). 0.5µg of total RNA was reverse transcribed using the iScript SuperMix reagent (Bio-Rad). Primers used for qPCR were as follows: *IL11* (human) Forward: 5'-TCT CTC CTG GCG GAC ACG-3'; Reverse: 5'-AAT CCA GGT TGT GGT CCC C-3'. GAPDH (human) Forward: 5'-GGA GCC AAA AGG GTC ATC AT-3'; Reverse: 5'-GTG ATG GCA TGG ACT GTG GT-3'. qPCR and fluorescence detection was performed using iQ SYBR Green Supermix (Bio-Rad) on an iCycler iQ real-time PCR detection system (Bio-Rad). Relative RNA levels were calculated from Ct values.

Patients

Serum and cDNA samples were obtained from ovarian cancer patients at Queen Mary Hospital from 1990 to 2016 and stored at the Department of Obstetrics & Gynaecology, The University of Hong Kong. Cases with chemosensitive and matched recurrent or chemoresistant tumor tissues were kept as formalin-fixed paraffin-embedded (FFPE) samples in the Department of Pathology at University of Hong Kong. All studies using human tissues were approved by the local institutional ethics committee (institutional review board reference No: UW 05-143 T/806 and UW 11-298). Written informed consent was received from patients prior to their inclusion in the study. The histological types, disease stages, and cancer cell contents in each FFPE sections were examined by the experienced pathologists. Written informed consent was given by the participants, and the use of the clinical specimens was approved by the local institutional ethics committee (institutional review board reference No: UW 05-143 T/806 and UW 11-298). The treatment of patients with ovarian cancer included total abdominal hysterectomy, bilateralsalpinpophorectomy (BSO), and

staging procedure for early disease, or debulking for advanced disease followed by adjuvant chemotherapy which consisted of either cisplatin or carboplatin alone, or in combination with paclitaxel. The overall survival rate was defined as the length of time from the diagnosis or surgery/chemotherapy to either disease progression, recurrence, death or the last follow-up date of the patients. According to our definition of platinum responses³⁹, platinum-sensitive was defined as patients who have a total responses to platinum-based therapy and no recurrence within 6 months, whereas platinum resistance means patients who had the recurrence occur within 6 months following the completion of platinum-based therapy. Patients with platinum refractory tumors that could not achieve a complete response after the platinum therapy were also as those with platinum-resistance.

Survival analysis in ovarian cancer

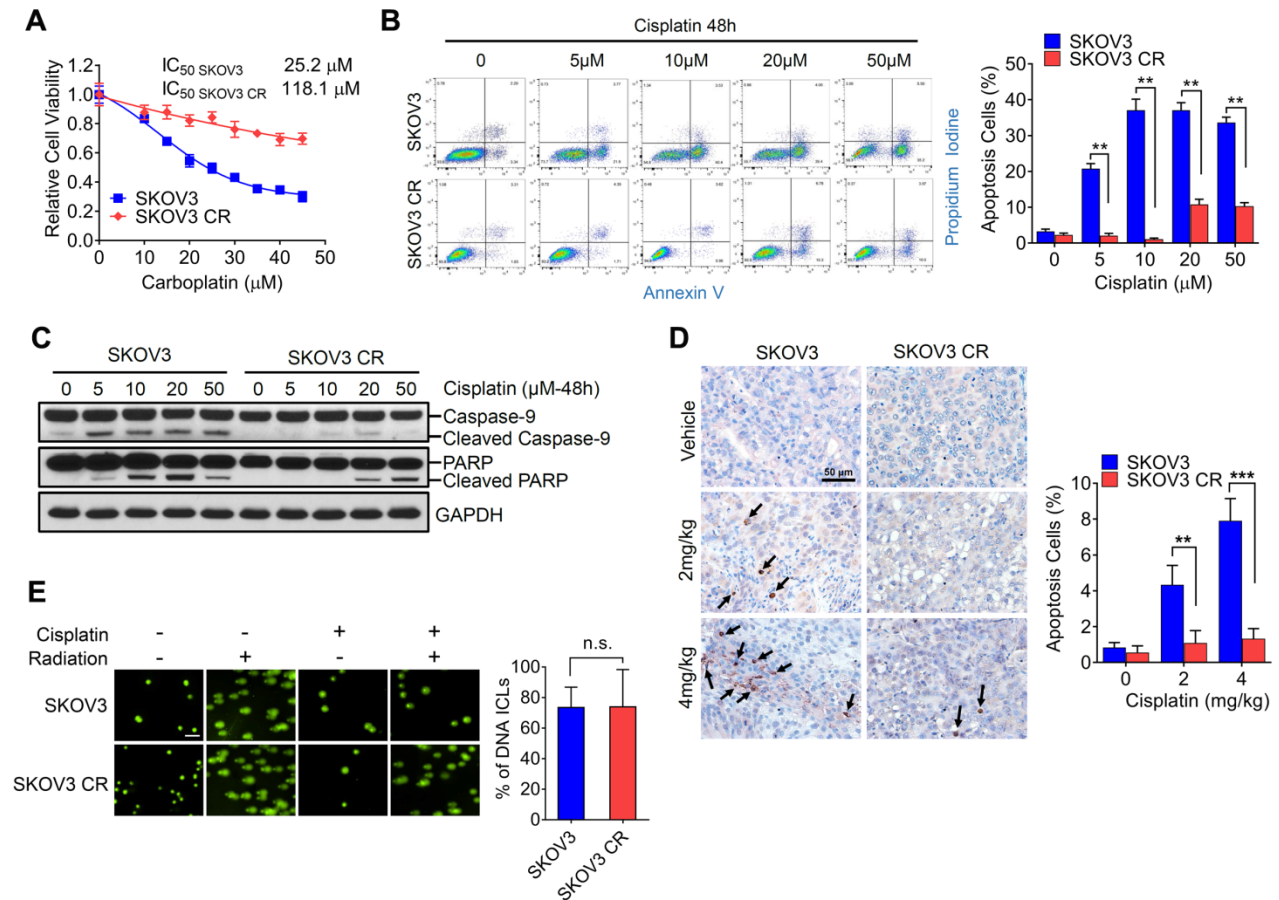
An open access online tool KM plotter (kmplot.com/analysis) was used to analyze the relationship between *IL11* and JAK2 signature gene expression from surviving ovarian cancer patient. 1816 patient in a 15 microarray dataset (TCGA n = 565, GSE 14764 n = 80, GSE 15622 n = 35, GSE 18520 n = 63, GSE 19829 n = 28, GSE 23554 n = 28, GSE 26193 n = 107, GSE 26712 n = 195, GSE 27651 n = 49, GSE 30161 n = 58, GSE 3419 n = 116, GSE 51373 n = 28, GSE 63885 n = 101, GSE 65986 n = 55, GSE 9891 n = 285) were included in the survival analysis. For *IL11* survival analysis, probe set 206924_at was used. Results were generated by the input “serous histology”, “suboptimal debulk”, and “contains platin chemotherapy” and by the “auto select best cutoff” option. For JAK2 signature gene set survival analysis, a multigene classifier was used with probes: 204531_s_at (BRCA1), 221918_at (CDK17), 214453_s_at (IFI44), 204439_at (IFI44L), 212918_at (RECQL), 209200_at (MEF2C), 203741_s_at (ADCY7), 203789_s_at (SEMA3C), 212507_at (TMEM131), 232057_at (SLC7A6OS), 209666_s_at (IKKA), 206584_at (LY96), 202100_at (RALB), 202450_s_at (PKND), 224842_at (SMG1), 228333_at (ZEB2), 203710_at (Insp3r1), 227031_at (SNX13), 235352_at (MR1), 205092_x_at (ZNF909), 206115_at (EGR3) and 204082_at. (PBX3). Results were

generated by using the input “contains platin chemotherapy” and by the “auto select best cutoff” options.

References

1. Zhu W, Lee CY, Johnson RL, Wichterman J, Huang R, DePamphilis ML. An image-based, high-throughput screening assay for molecules that induce excess DNA replication in human cancer cells. *Mol Cancer Res* **2011**;9:294-310
2. Sun W, Tanaka TQ, Magle CT, Huang W, Southall N, Huang R, *et al.* Chemical signatures and new drug targets for gametocytocidal drug development. *Sci Rep* **2014**;4:3743
3. Griner LAM, Guha R, Shinn P, Young RM, Keller JM, Liu D, *et al.* High-throughput combinatorial screening identifies drugs that cooperate with ibrutinib to kill activated B-cell-like diffuse large B-cell lymphoma cells. *Proceedings of the National Academy of Sciences of the United States of America* **2014**;111:2349-54
4. Karaman MW, Herrgard S, Treiber DK, Gallant P, Atteridge CE, Campbell BT, *et al.* A quantitative analysis of kinase inhibitor selectivity. *Nat Biotechnol* **2008**;26:127-32
5. Moretti S, Armougom F, Wallace IM, Higgins DG, Jongeneel CV, Notredame C. The M-Coffee web server: a meta-method for computing multiple sequence alignments by combining alternative alignment methods. *Nucleic Acids Res* **2007**;35:W645-8
6. Forbes SA, Beare D, Gunasekaran P, Leung K, Bindal N, Boutselakis H, *et al.* COSMIC: exploring the world's knowledge of somatic mutations in human cancer. *Nucleic Acids Res* **2015**;43:D805-11
7. Zhu W, Chen Y, Dutta A. Rereplication by depletion of geminin is seen regardless of p53 status and activates a G2/M checkpoint. *Mol Cell Biol* **2004**;24:7140-50

Supplementary Figure S1



Supplementary Figure 1. Establishment of platinum resistant ovarian cancer cell lines and identification of compounds that overcome cisplatin resistance

(A) Viability of SKOV3 and SKOV3 CR cells treated with increasing concentrations of carboplatin for 5 days. Data are represented as mean \pm SD. The IC₅₀ values represent the mean of two independent experiments performed in triplicate.

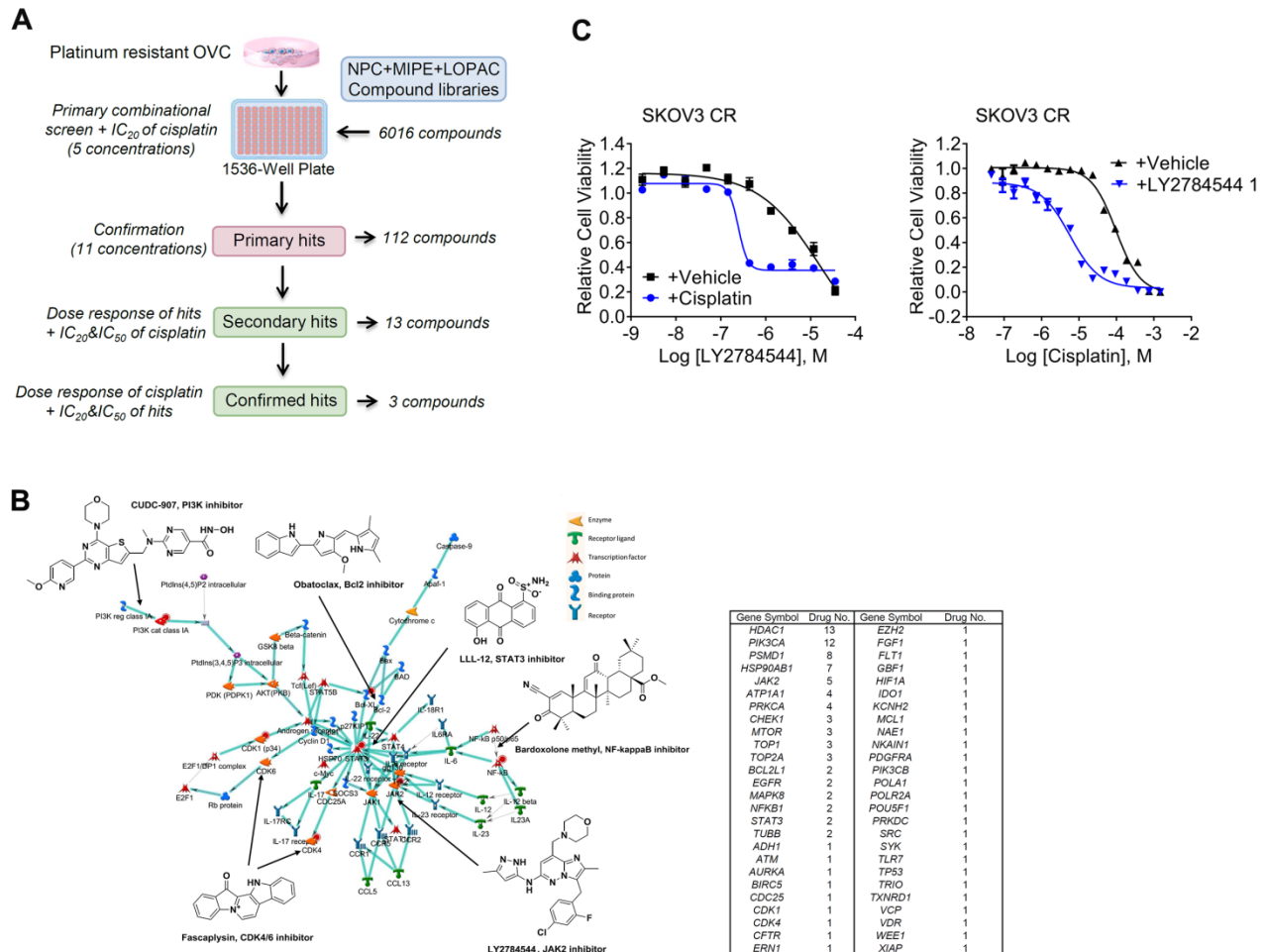
(B) Representative flow cytometry dot plots (left) and quantification (right) of SKOV3 and SKOV3 CR cells treated with cisplatin for 48 hr and analyzed for Annexin V and Propidium Iodide staining by flow cytometry. ** $P < 0.01$ by Student's t-test.

(C) The effect of cisplatin on the proteolytic activation of caspase-9 and cleavage of PARP in the parental SKOV3 and SKOV3 CR cells.

(D) Representative images (left) and quantification (right) of TUNEL staining of SKOV3 and SKOV3 CR tumor xenografts after 4 days of treatment with cisplatin (2mg/kg or 4mg/kg twice per week for two weeks); n = 4 mice/group. Scale bar, 50 μ m. **p < 0.01, ***p < 0.001 by Student's t-test; arrows indicate apoptotic cells.

(E) Representative images (left) and quantification (right) from the modified comet assay performed after SKOV3 and SKOV3 CR cells had been treated with cisplatin for 2 hr followed by an irradiation treatment at 20 Gy. DNA ICLs: DNA interstrand crosslinking. Scale bar, 100 μ m. n.s. means not significant by Student's t-test

Supplementary Figure S2



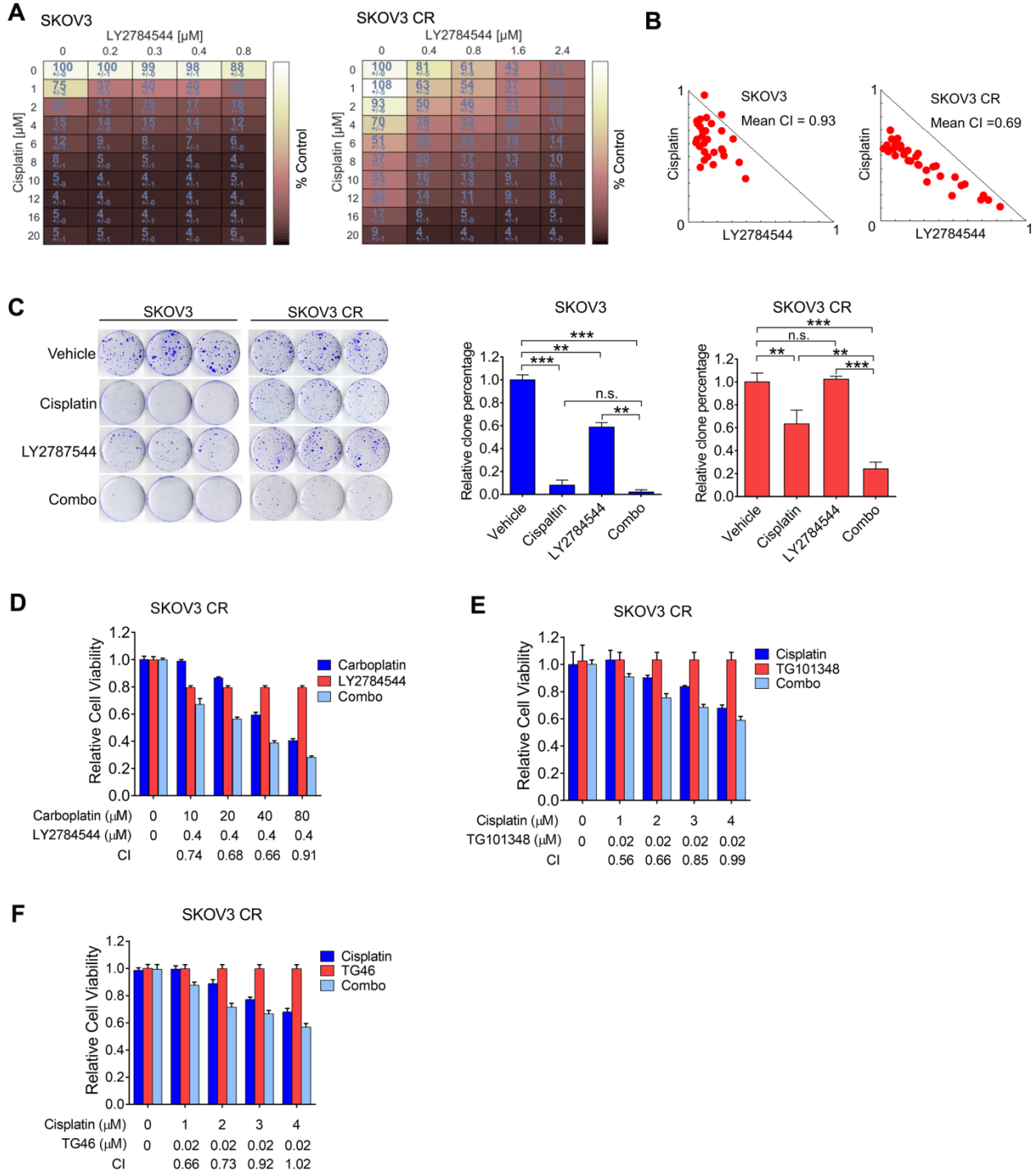
Supplementary Figure 2. Identification of compounds that resensitizes platinum drug by qHTCS

(A) Flow chart for qHTCS compound screening using platinum resistant ovarian cancer cells. The criteria for compound selection and the number of compounds included at each step are listed.

(B) Principal active 112 compounds from primary qHTCS screening, their mechanism of action, and their chemical genomic association in the top enriched network in MetaCore.

(C) LY2784544 and its dose-dependent effects on cells in the presence of cisplatin measured by qHTCS . Data are represented as mean \pm SEM. The mechanism of action of the compounds are list in the table.

Supplementary Figure S3



Supplementary Figure 3. LY2784544 synergies with platinum drugs by JAK2 inhibitors

(A) Matrix representation of viability assay in SKOV3 (left) and SKOV3 CR (right) cells treated with indicated concentrations of cisplatin and LY2784544 (n=3).

(B) Isobologram analysis of the effects of cisplatin and LY2784544 at multiple concentrations on SKOV3 and SKOV3 CR cells in (A). Results are the mean values of three independent experiments performed in triplicate. CI, combination index.

(C) Colony formation by SKOV3 and SKOV3 CR cells 14 days after they have been treated with 0.5 μ M cisplatin and/or 0.1 μ M LY2784544. Colonies were stained with crystal violet. Data are represented as mean \pm SD from three independent experiments performed in triplicate. **p < 0.01, ***p < 0.00, n.s. means not significant by one-way ANOVA,

(D) The synergistic effects of LY2784544 and carboplatin on SKOV3 CR cells. The CI values are presented below the bars. Data are represented as mean \pm SD from three independent experiments performed in triplicate.

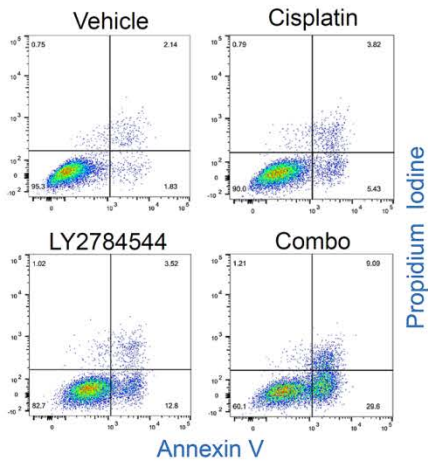
(E) The synergistic effects of the JAK2 inhibitor TG101348 and cisplatin on SKOV3 CR cells. The CI values are presented below the bars. Data are represented as mean \pm SD from three independent experiments performed in triplicate.

(F) The synergistic effects of the JAK2 inhibitor TG46 and cisplatin on SKOV3 CR cells. The CI values are presented below the bars. Data are represented as mean \pm SD from three independent experiments performed in triplicate.

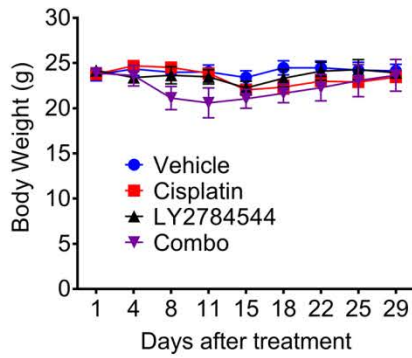
In all panels of this figure, CI < 1 indicates synergism, CI = 1 indicates additive effect, and CI > 1 indicates antagonism.

Supplementary Figure S4

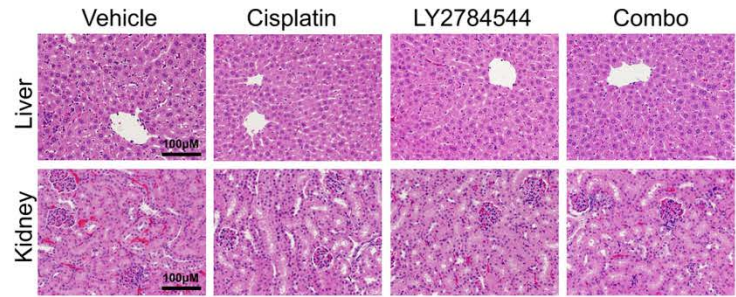
A



B



C



D

KINOMEScan (percent control)			
ABL1	0.2	JAK1	0.5
ALK	0.8	JAK2	0.15
PRKAA2	0.65	KIT	0.35
NUAK1	0.35	LTK	0.2
AURKB	0.4	MAP3K2	0.35
AXL	0.95	MAP2K3	0.85
BLK	0.25	MERTK	0.3
BMPR1B	0.25	MYLK4	0.4
CDKL2	0.5	PDGFRB	0.1
CSF1R	0.1	PHKG1	0.6
DCLK2	0.45	PLK4	0.1
DDR1	0.3	SLK	0.55
EPHA5	0.5	NUAK2	0.8
EPHA7	0.55	SRPK1	0.05
MAPK7	0.05	NTRK2	0.15
PTK2	0.2	NTRK3	0.1
FGFR1	0.2	TYK2	0.45
FGFR2	0.75	KDR	0.4
FLT3	0.45	PIK3C3	0.35
FLT4	0.35	MAP3K19	0.65
HCK	0.65		

Supplementary Figure 4. LY2784544 *in vitro* kinase assay and *in vivo* toxicity

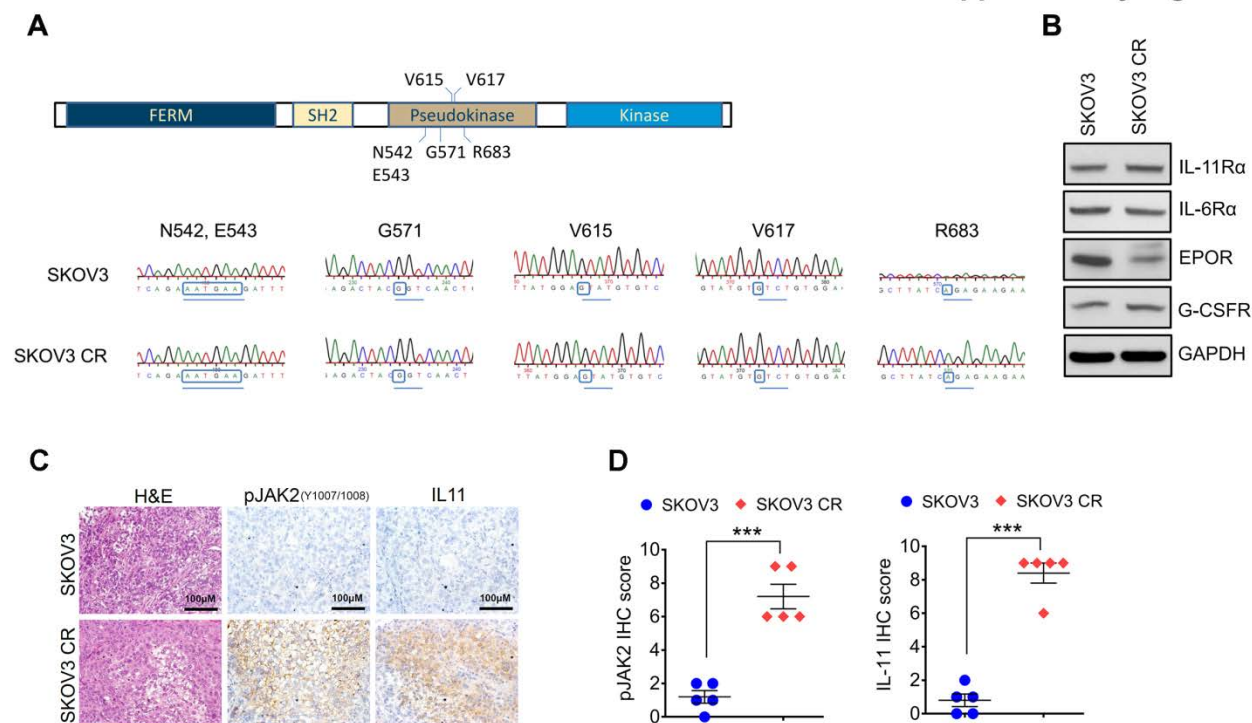
(A) Representative flow cytometry plots of Apoptosis of SKOV3 CR cells treated with vehicle, 3 μ M LY2784544, 5 μ M cisplatin, or the combination (Combo) for 48 hr.

(B) Body weights of SKOV3 tumor-bearing mice during treatment as in Fig. 3g. Data are represented as means \pm SEM, $n = 6$ mice/group.

(C) Representative histopathology of liver and kidney collected from mice treated as in Fig. 3i. Scale bar, 100 μ m.

(D) Binding interactions of 43 hits reported as ≤ 1 % percent of control in KinomeScan assay. The lower numbers indicate stronger interactions by LY2784544.

Supplementary Figure S5



Supplementary Figure 5. JAK2 gene analysis and receptor expression

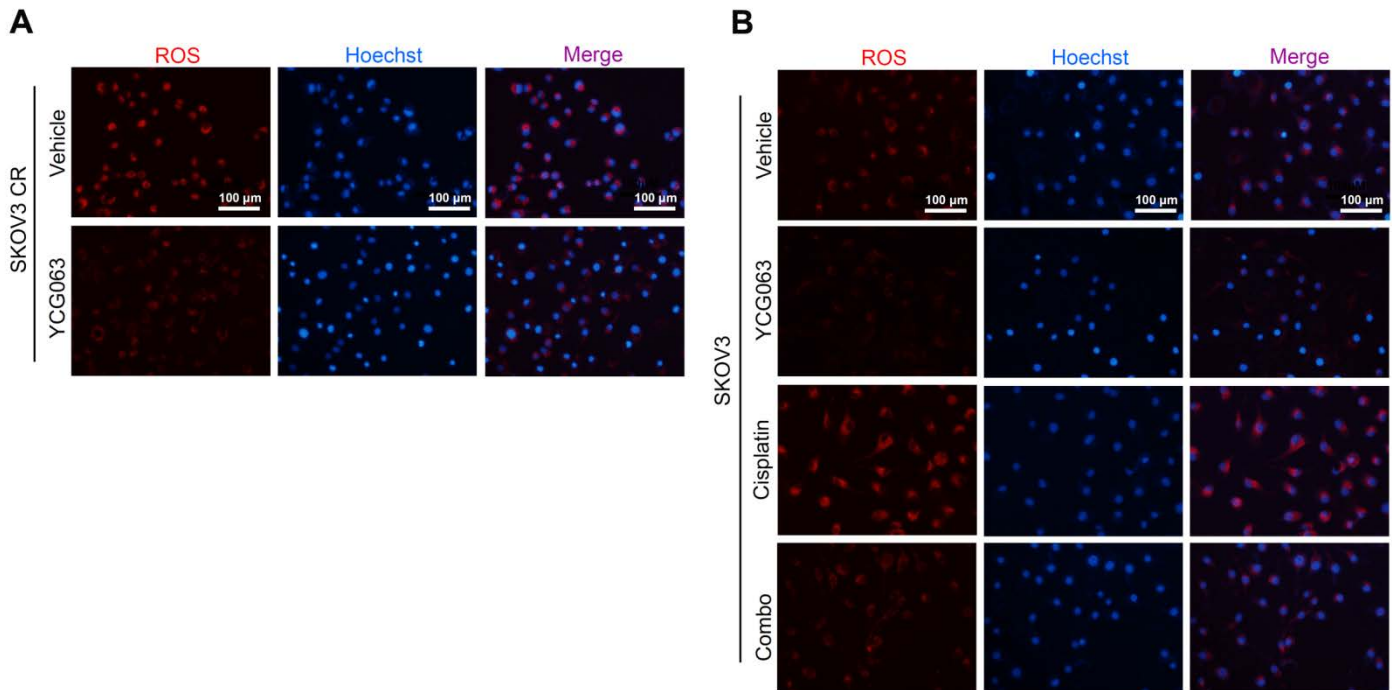
(A) Comparison of high frequent point mutations in SKOV3 and SKOV3 CR.

(B) Immunoblotting of JAK2-related receptors in SKOV3 and SKOV3 CR cells.

(C) Representative H&E and IHC images of SKOV3 and SKOV3 CR tumor xenografts. Scale bar, 100 μ m.

(D) Quantification of IHC staining for pJAK2 and IL-11 in tumors as in (C). Data represented as means \pm SEM. *** $p < 0.001$ by Student's t-test.

Supplementary Figure S6

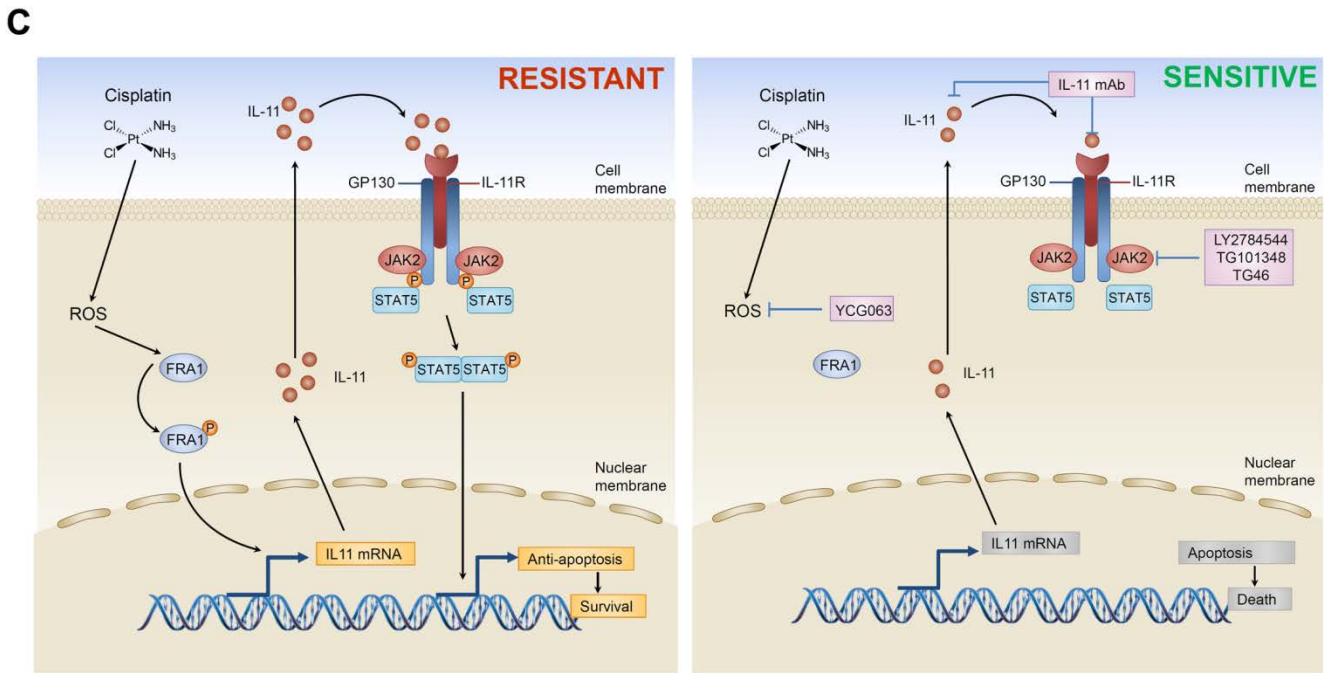
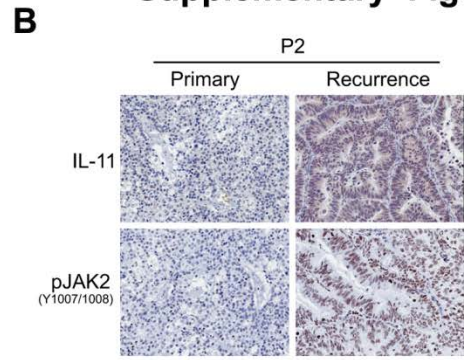
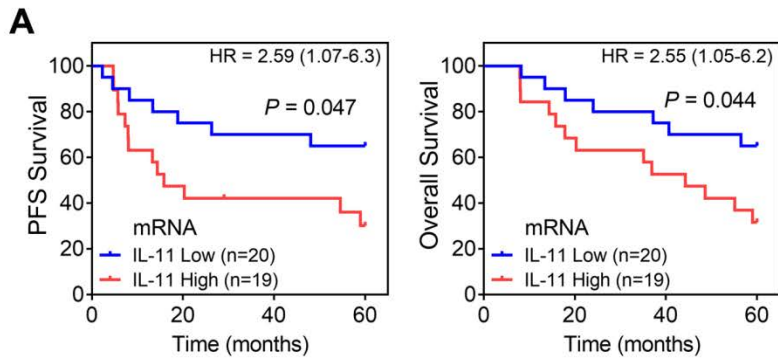


Supplementary Figure 6. Effects on cisplatin-induced IL-11 secretion by ATR inhibitor or ROS inhibitor

(A) Representative images of reactive oxygen species (ROS) production in SKOV3 CR cells in the absence or presence of YCG063 (20 μ M) for 24 hr. Scale bar, 100 μ m.

(B) Representative images of reactive oxygen species (ROS) production in SKOV3 cells after treated by vehicle, YCG063 (20 μ M), cisplatin (1 μ M) or both (Combo) for 24 hr. Scale bar, 100 μ m.

Supplementary Figure S7



Supplementary Figure 7. IL-11 and JAK2 pathway in platinum drug resistant ovarian cancer patients

(A) Kaplan–Meier survival curves showing 5-year PFS rate (left panel) and OS rate (right panel) of 39 ovarian cancer patients as show in Fig.8g, who were stratified by *IL11* mRNA levels by median cutoff); log-rank (Mantel-Cox), *P* values and HRs are shown.

(B) Representative IHC images of IL-11 and p-JAK2 in platinum sensitive and recurrent tumor samples from one patient (P2).

(C) Schematics of IL-11-JAK2-mediated pathway in the regulation of platinum drug resistance in ovarain cancer. Left: ROS-mediated activation of IL-11-JAK2 pathway leads to platinum drug resistance in ovarian cancer. Right: inhibition of JAK2 or IL-11 resensitizes platinum drug resistant ovarian cancer cells to platinum drugs.